© 2018. Published by The Company of Biologists Ltd | Development (2018) 145, dev143107. doi:10.1242/dev.143107

RESEARCH ARTICLE

Head formation requires Dishevelled degradation that is mediated by March2 in concert with Dapper1

Hyeyoon Lee*,, Seong-Moon Cheong‡,**, Wonhee Han, Youngmu Koo, Saet-Byeol Jo, Gun-Sik Cho§, Jae-Seong Yang¶, Sanguk Kim and Jin-Kwan Han‡‡**

ABSTRACT

Dishevelled (Dvl/Dsh) is a key scaffold protein that propagates Wnt signaling essential for embryogenesis and homeostasis. However, whether the antagonism of Wnt signaling that is necessary for vertebrate head formation can be achieved through regulation of Dsh protein stability is unclear. Here, we show that membrane-associated RING-CH2 (March2), a RING-type E3 ubiquitin ligase, antagonizes Wnt signaling by regulating the turnover of Dsh protein via ubiquitin-mediated lysosomal degradation in the prospective head region of *Xenopus*. We further found that March2 acquires regional and functional specificities for head formation from the Dsh-interacting protein Dapper1 (Dpr1). Dpr1 stabilizes the interaction between March2 and Dsh in order to mediate ubiquitylation and the subsequent degradation of Dsh protein only in the dorso-animal region of *Xenopus* embryo. These results suggest that March2 restricts cytosolic pools of Dsh protein and reduces the need for Wnt signaling in precise vertebrate head development.

KEY WORDS: Wnt signaling, Dishevelled, March2, Dapper1, Head formation, *Xenopus*

INTRODUCTION

Wnt signaling governs various cellular processes, including cell proliferation, differentiation, migration, establishment of polarity and stem cell self-renewal. Dysregulation of Wnt signaling causes developmental defects and human diseases, including cancer (Barker and Clevers, 2006; Clevers, 2006; Logan and Nusse, 2004; MacDonald et al., 2009). Wnt signaling is divided into the β-catenin-dependent canonical pathway and β-catenin-independent non-canonical pathway. In the canonical Wnt pathway, binding of Wnt ligands to the LDL receptor-related protein 6 (LRP6) co-receptor and Frizzled (Fz) receptor induces aggregation and phosphorylation of LRP6 through Dsh-mediated scaffold formation (Bilic et al., 2007; Gao and Chen, 2010; Sheng et al., 2014). Upon ternary LRP6-Wnt-Fz complex formation, Dsh binds to Axin, which recruits glycogen synthase kinase 3β (GSK3β) to phosphorylate LRP6 (Bilic et al., 2007). Inhibition of GSK3β by the phospho-LRP6-containing activated receptor complex protects β-catenin from proteasomal degradation (Logan and Nusse, 2004; MacDonald et al., 2009). Consequently, β-catenin accumulates and interacts with T-cell factor/lymphoid-enhancer factor (TCF/LEF) in the nucleus, thereby initiating transcription.

During vertebrate development, the canonical Wnt pathway plays a crucial role in head formation (Glinka et al., 1997; Kiecker and Niehrs, 2001; Yamaguchi, 2001). Proper head formation requires inhibition of the canonical Wnt pathway by various Wnt antagonists, including Dickopf-1 (Dkk1) and secreted Fz-related proteins (sFRPs), which are secreted from the head organizer of gastrula embryos and thereby maintain a low level of Wnt signaling at the putative anterior region of embryos (De Robertis and Kuroda, 2004; Niehrs, 2004). A recent study revealed that the transmembrane protein Tiki is required for head formation via cleavage and inactivation of Wnt ligands (Zhang et al., 2012). These well-identified Wnt antagonists involved in head formation collectively exert their roles by regulating perimembranous or extracellular events in Wnt activation, including Wnt ligand binding to receptors or modification of the ligand itself. However, whether antagonism of the Wnt signal necessary for head formation can be achieved through regulation of Dsh protein stability has not been extensively investigated.

Membrane-associated RING-CH (March) proteins are recently identified members of the mammalian E3 ubiquitin ligase family (Bartee et al., 2004). It is known that one member of this family, March2, is localized to endosomal vesicles as well as to the plasma membrane, and binds to syntaxin 6, which is involved in endosomal trafficking (Nakamura et al., 2005). In addition, March2 is involved in downregulation of discs large 1 (Dlg-1), a polarity-determining protein containing three PDZ domains (Cao et al., 2008). Recent research also suggests that March2 regulates lysosomal sorting of carvedilol-bound β2-adrenergic receptors via ubiquitylation (Han et al., 2012). However, the role of March2 during development and its targeted developmental signal have not yet been elucidated.

In this study, we have defined March2 as a novel ubiquitin ligase that targets *Xenopus* Dsh for ubiquitin-mediated degradation, thereby antagonizing Wnt signaling and regulating head formation. We have also addressed the molecular details of the mechanism by which March2 inhibits Wnt, discovering that March2 interacts with and degrades Dsh in concert with another Dsh scaffold protein, Dapper1 (Dpr1/DACT1), in *Xenopus* embryos. Dpr1 has been identified as a Dsh-interacting protein that inhibits Wnt signaling by mediating Dsh degradation (Cheyette et al., 2002; Zhang et al., 2006). Interestingly, however, how Dpr1, a scaffold protein that lacks intrinsic enzymatic activity, regulates the stability of Dsh protein remains unclear. Although several E3 ubiquitin ligases have been suggested to regulate Dsh stability (Angers et al., 2006; Chan et al., 2006; Ganner et al., 2009; Miyazaki et al., 2004;

Department of Life Sciences, Pohang University of Science and Technology, 77 Cheongam-Ro, Nam-Gu, Pohang, Gyeongbuk, 37673, Korea.
*Present address: Division of Molecular Embryology, DKFZ-ZMBH Alliance, Deutsches Krebsforschungszentrum (DKFZ), 69120 Heidelberg, Germany.
‡Present address: Department of Neurology, The F.M. Kirby Neurobiology Center, Boston Children's Hospital, Harvard Medical School, Boston, MA 02115, USA.
§Present address: Laboratory of Stem Cells, NEXEL, Seoul, Republic of Korea.
¶Present address: EMBL/CRG Systems Biology Research Unit, Center for Genomic Regulation, Dr. Aiguader 88, Barcelona, Spain.
**These authors contributed equally to this work

‡‡Author for correspondence (jkh@postech.ac.kr)

J.-K.H., 0000-0001-6909-3557

Received 1 August 2016; Accepted 21 February 2018

Development (2018) 145, dev143107. doi:10.1242/dev.143107

Zhang et al., 2014), none seems to be directly linked with Dpr1, suggesting the possible involvement of an unidentified, genuine E3 ubiquitin ligase that downregulates Dsh protein in concert with Dpr1. Our new findings suggest that March2 is this novel E3 ubiquitin ligase and exerts this role in *Xenopus* head formation.

RESULTS

Cloning and expression of March2 in *Xenopus*

To fully understand the regulatory mechanism and function of Dsh during *Xenopus* embryogenesis, we sought to identify new binding partners of Dsh protein that might regulate Wnt signaling in *Xenopus*. To achieve this we performed a computational screening analysis based on the predicted ligand selectivity of the PDZ domain (Kim et al., 2012) of Dsh with *Xenopus* proteins that contain PDZ-binding motifs. Among the putative Dsh binding proteins, *Xenopus* March2, the RING-type E3 ubiquitin ligase, was highly scored but its function during vertebrate development has not previously been reported (Table S2). Thus, we identified and cloned the cDNA for the *Xenopus* orthologue of March2, which consists of 741 nucleotides encoding a protein of 246 amino acids (Gene ID: 495994) that contains a RING (really important new gene) E3-ligase domain, two transmembrane domains and a C-terminal PDZ-binding motif (Fig. S1A). The encoded protein showed high similarity to other vertebrate orthologs (human, 86%; mouse, 79%; chick, 93%; zebrafish, 89%).

Before verifying the potential binding of March2 to Dsh, we analyzed the spatiotemporal expression of March2 transcripts and protein. Both maternal and zygotic expression of endogenous March2 transcripts and protein were assessed by RT-PCR and western blotting throughout *Xenopus* development (Fig. S1B,U). *In situ* hybridization showed that March2 transcripts were strongly enriched at the animal hemisphere in blastula stages (st. 3 and st. 9) (Fig. S1C,D). As gastrulation proceeded (st. 10 and st. 11) (Fig. S1E-J), March2 transcripts became ubiquitously expressed, but also showed noteworthy expression in the dorsal marginal zone (DMZ), including the head organizer (Fig. S1G,J,T). During neurulation (st. 12 to st. 20), March2 transcripts were detectable in the anterior neural plate and neural plate border region. At later times, March2 transcripts were exclusively found in the head region and heart field (st. 27 and st. 36) (Fig. S1Q-S). These data suggest that March2 is consistently expressed during *Xenopus* embryogenesis and may play a role in head development.

March2 interacts with Dsh

To validate the potential binding of *Xenopus* March2 with Dsh, which was suggested by our computational analysis, we performed co-immunoprecipitation (co-IP) analyses. Our results clearly showed that March2 interacts with Dsh ectopically (Fig. 1A) and endogenously (Fig. 1B) in HEK293FT cells (Fig. 1B). In addition, confocal imaging revealed that cytosolic puncta of March2 protein colocalized with Dsh in *Xenopus* animal caps (Fig. 1C) and human cells (Fig. 1D), providing additional evidence that these proteins can associate with each other. To further characterize the binding of March2 with Dsh, we compared binding of Dsh deletion-mutant forms lacking each conserved domain (DIX, PDZ and DEP) with full-length March2 (Fig. 1E). Our results showed that Dsh binding to March2 was completely lost in a mutant lacking the DEP domain, and was dramatically weakened in a mutant lacking the PDZ domain. In contrast, deletion of the DIX domain had no effect on the binding ability or affinity of Dsh for March2 (Fig. 1E). These results support the interpretation that both DEP and PDZ domains of Dsh are required for the interaction with March2, with the DEP domain playing a more prominent role (Fig. 1E).

To identify the March2 domain responsible for Dsh binding, we next constructed two deletion-mutant forms of March2, one lacking the C-terminal region containing the PDZ-binding motif (Mar2ΔC) and a second lacking the N-terminal region containing the RING domain (Mar2ΔN), and analyzed the mutants for their ability to bind Dsh (Fig. 1F). Our result revealed that Dsh bound to Mar2ΔN but not to Mar2ΔC, indicating that the C-terminal region of March2 interacts with Dsh.

Since our screening analysis was based solely on the possibility that the PDZ-binding motif consists of four amino acids at the C terminus of March2 that specifically interact with Dsh, we next directly tested whether this motif itself is indeed responsible for Dsh binding. Unexpectedly, co-IP analyses revealed that deletion of the PDZ-binding motif from March2 did not prevent March2 from binding Dsh (data not shown). This unanticipated result implies that the C-terminal region of March2 that includes amino acids 200-246, rather than a single PDZ-binding motif, is important for Dsh binding. Nonetheless, taken together, these results suggest that March2 is a new Dsh-interacting partner that binds through association of the C-terminal region of March2 with both PDZ and DEP domains of Dsh.

March2 regulates the stability of Dsh protein in *Xenopus*

As March2 is known as an E3-ubiquitin ligase that mediates the ubiquitylation and subsequent degradation of its targets (Cao et al., 2008; Cheng and Guggino, 2013; Han et al., 2012), we hypothesized that March2 binding to Dsh serves to regulate the stability of Dsh protein in *Xenopus*. To test this hypothesis, we analyzed the effects of dose-dependent expression of March2 on the protein level of Dsh in *Xenopus* (Fig. 2A). Our result showed increasing amounts of March2 remarkably decreased Dsh protein levels (Fig. 2A). This ability of March2 to reduce Dsh protein was maintained from late blastula to early gastrula stages (Fig. S2A). Conversely, knockdown of March2 by injecting three respective March2 antisense morpholino oligonucleotides (Mar2MO, Mar2MO2 and Mar2MO3), which efficiently depleted March2 protein expression in *Xenopus* (Figs S6B,C and S7B), increased Dsh protein level in a dose-dependent manner, indicating that decreasing March2 function stabilizes Dsh protein. Mar2MO-induced increase in Dsh protein was attenuated by co-expression of the MO-resistant form of March2 mRNA, which lacks 5′UTR region to which the MOs bind (Fig. 2B, Figs S6D and S7C). We then analyzed transcript levels of Dsh following injection with increasing amounts of either March2 mRNA or Mar2MO to eliminate the possibility that the effect of March2 overexpression or knockdown on Dsh stability occurred through regulation of *Dsh* transcription. RT-PCR analyses showed that neither overexpression nor knockdown of March2 affected *Dsh* transcription (Fig. S2B,C).

As co-IP analysis (Fig. 1E) showed that PDZ and DEP domains of Dsh are important for the binding of March2, we next asked whether March2 is unable to degrade Dsh mutant proteins lacking either PDZ or DEP domains. Expression of March2 in *Xenopus* did not affect the Dsh mutants lacking PDZ or DEP domains but effectively reduced DIX-domain-deleted forms of Dsh protein, though not as much as the wild type (Fig. 2C).

To further elucidate whether the reduction of Dsh stability upon March2 expression was attributable to enhanced ubiquitylation of Dsh by March2 E3-ubiquitin ligase activity, we generated a mutant form of March2 (March2CS) that lacks this activity by virtue of a substitution of serine residues for four crucial cysteine residues within the RING domain of March2 (Cao et al., 2008) and analyzed

Development (2018) 145, dev143107. doi:10.1242/dev.143107

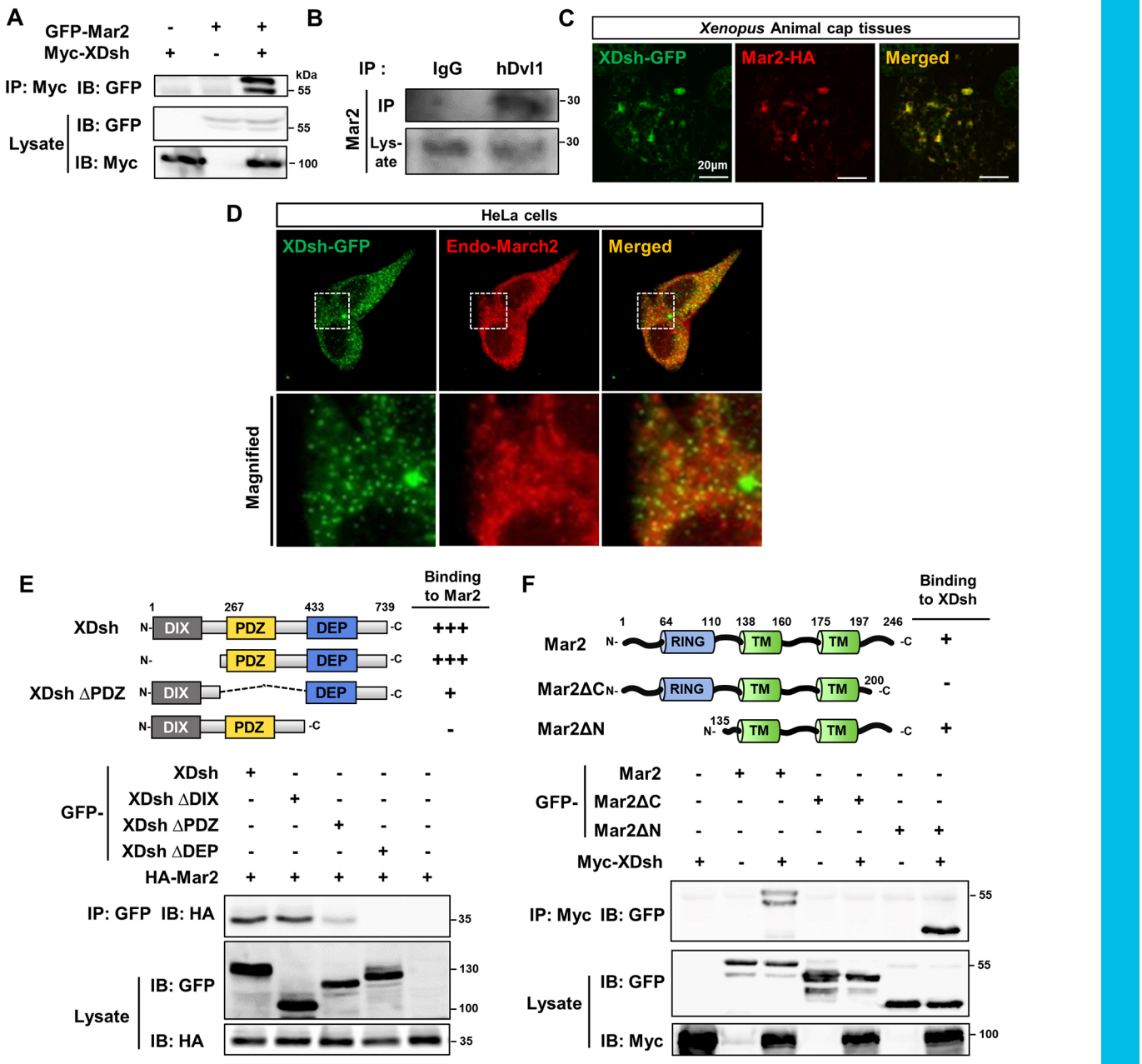

Fig. 1. *Xenopus* March2 interacts with Dsh. (A) Co-immunoprecipitation analysis with GFP-March2 and Myc-XDsh in HEK293FT cells. (B) Interaction of endogenous human Dvl1 with March2 in HEK293FT cells. Immunoprecipitation with anti-IgG antibody used as a negative control. (C) *Xenopus* animal caps injected with GFP-XDsh (500 pg) and HA-Mar2 (250 pg) mRNAs were immunostained and analyzed by confocal microscopy. (D) HeLa cells transfected with GFP-XDsh were stained with anti-GFP and anti-March2 antibody and analyzed by confocal microscopy. (E) Schematics of the various XDsh deletion mutants (top) used for co-immunoprecipitation analysis (bottom). Note that the PDZ and DEP domains of Dsh are required for the March2 interaction in HEK293FT cells. (F) Schematics of full-length March2, C-terminus-deleted and N-terminus-deleted mutant forms (top) and co-immunoprecipitation results (bottom) showing that the C-terminal region of March2 is important for the interaction with Dsh.

its effect on the Dsh protein (Fig. 2D). Our results showed that March2CS did not reduce the Dsh protein levels (Fig. 2D).

We next carried out *in vivo* ubiquitylation assays (Fig. 2E) using inhibitors of proteasomal (MG132) and lysosomal degradation (bafilomycin A1 and leupeptin) simultaneously, because previous reports have shown that the stability of Dsh protein can be regulated by both proteasome- and lysosome-dependent pathways (Angers et al., 2006; Chan et al., 2006; Ganner et al., 2009; Gao et al., 2010; Miyazaki et al., 2004; Zhang et al., 2006, 2014). We found that wild-type March2, but not March2CS, dramatically induced Dsh poly-ubiquitylation. In addition, March2 depletion led to a loss of Dsh poly-ubiquitylation (Fig. 2F). Collectively, these results indicate that March2 acts through interactions with PDZ and DEP domains of Dsh to specifically target Dsh protein for poly-ubiquitination-dependent degradation during *Xenopus* embryogenesis.

March2 targets Dsh to the lysosomal degradation pathway in *Xenopus*

We next asked to which pathway does March2 guide poly-ubiquitylated Dsh proteins for degradation? To address this question, we performed *in vivo* ubiquitylation assays in *Xenopus* (Fig. 3A,B) to determine the pathway responsible for March2-

Development (2018) 145, dev143107. doi:10.1242/dev.143107

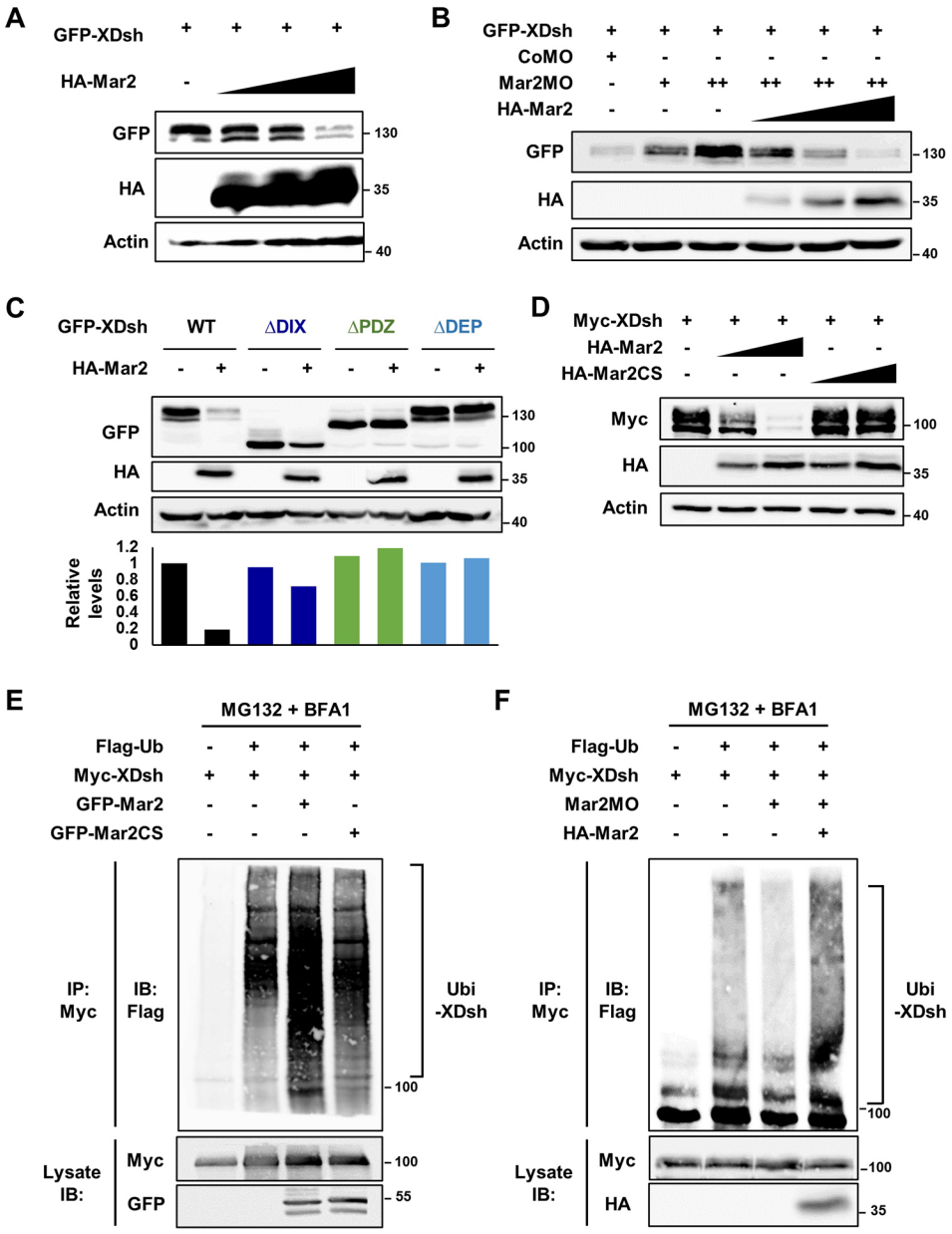

Fig. 2. *Xenopus* March2 induces the ubiquitylation-mediated degradation of Dsh. (A) March2 decreases Dsh protein in *Xenopus*. HA-Mar2 mRNA (250 pg, 500 pg, 1 ng) along with 200 pg of GFP-XDsh mRNA were injected and analyzed by western blotting at stage 10.5. (B) Mar2MO stabilizes Dsh protein. Mar2MO (40, 80 ng) was injected with 150 pg of GFP-XDsh mRNA. Co-injection of 250, 500 pg and 1 ng of March2 mRNA along with 80 ng of Mar2MO gradually reduced Dsh levels again. (C) DEP and PDZ domains of Dsh are required for March2 mediated Dsh degradation. All forms of GFP-XDsh mRNA, 250 pg; HA-Mar2 mRNA, 1 ng. (D) March2CS cannot degrade Dsh. The amounts of mRNAs: Myc-XDsh, 250 pg; HA-Mar2 WT and CS, 500 pg and 1 ng, respectively. (E,F) *In vivo* ubiquitylation assays in *Xenopus*. Dsh protein was pulled down and poly-ubiquitylated Dsh protein was detected. The amounts of injected mRNAs: Flag-Ub, 2 ng; Myc-XDsh, 2 ng; GFP-Mar2 WT and CS, 1 ng; Mar2MO, 40 ng.

dependent Dsh degradation. These analyses revealed that March2 mediated poly-ubiquitylation of Dsh protein was increased by treatment with bafilomycin A1 (Fig. 3A) or leupeptin (Fig. 3B), but not by MG132 (Fig. 3A), supporting the notion that March2-mediated ubiquitylation targets Dsh to the lysosomal pathway. In addition, we monitored the subcellular localization of March2 protein in *Xenopus* animal cap tissues (Fig. 3C) and human culture cells (Fig. 3D). The cytosolic puncta of March2 proteins was strongly colocalized with the late endosome/lysosomal marker protein Rab7 and Lamp1 (Fig. 3C,D), but not with the early endosome marker EEA1 (Fig. 3C). Taken together, these results demonstrate that March2 regulates the stability of Dsh protein in *Xenopus* by mediating its poly-ubiquitylation and subsequent lysosomal degradation.

March2 antagonizes the canonical Wnt signaling pathway

Given that the canonical Wnt pathway requires Dsh as a key scaffold protein for multiple steps in the signaling process, including Wnt-Fz-LRP5/6 receptor complex formation and aggregation (Gao and Chen, 2010; Sheng et al., 2014), LRP5/6 phosphorylation and β-catenin stabilization (Bilic et al., 2007), we next investigated the evident possibility that March2 is involved in the Wnt pathway and antagonizes various signaling steps by restricting the Dsh protein pool during *Xenopus* embryogenesis. To examine the effects of loss or gain of March2 function on Wnt-dependent transcriptional activity, we performed reporter assays in *Xenopus* embryos using a TOP-flash reporter containing TCF-binding sites. Knockdown of March2 boosted Wnt-dependent transcriptional activity (Fig. 4A), whereas ectopic expression of March2 inhibited Dsh-induced transcriptional activity (Fig. 4D). However, March2 expression could not affect the transcriptional activity induced by β-catenin, indicating that March2 antagonizes Wnt signaling and functions upstream of β-catenin (Fig. 4D). In addition, western blot analyses revealed that knockdown of March2 promoted activation of β-catenin (Fig. 4B, Figs S6E and S7D) as well as phosphorylation of LRP6 (Fig. 4B), whereas

Development (2018) 145, dev143107. doi:10.1242/dev.143107

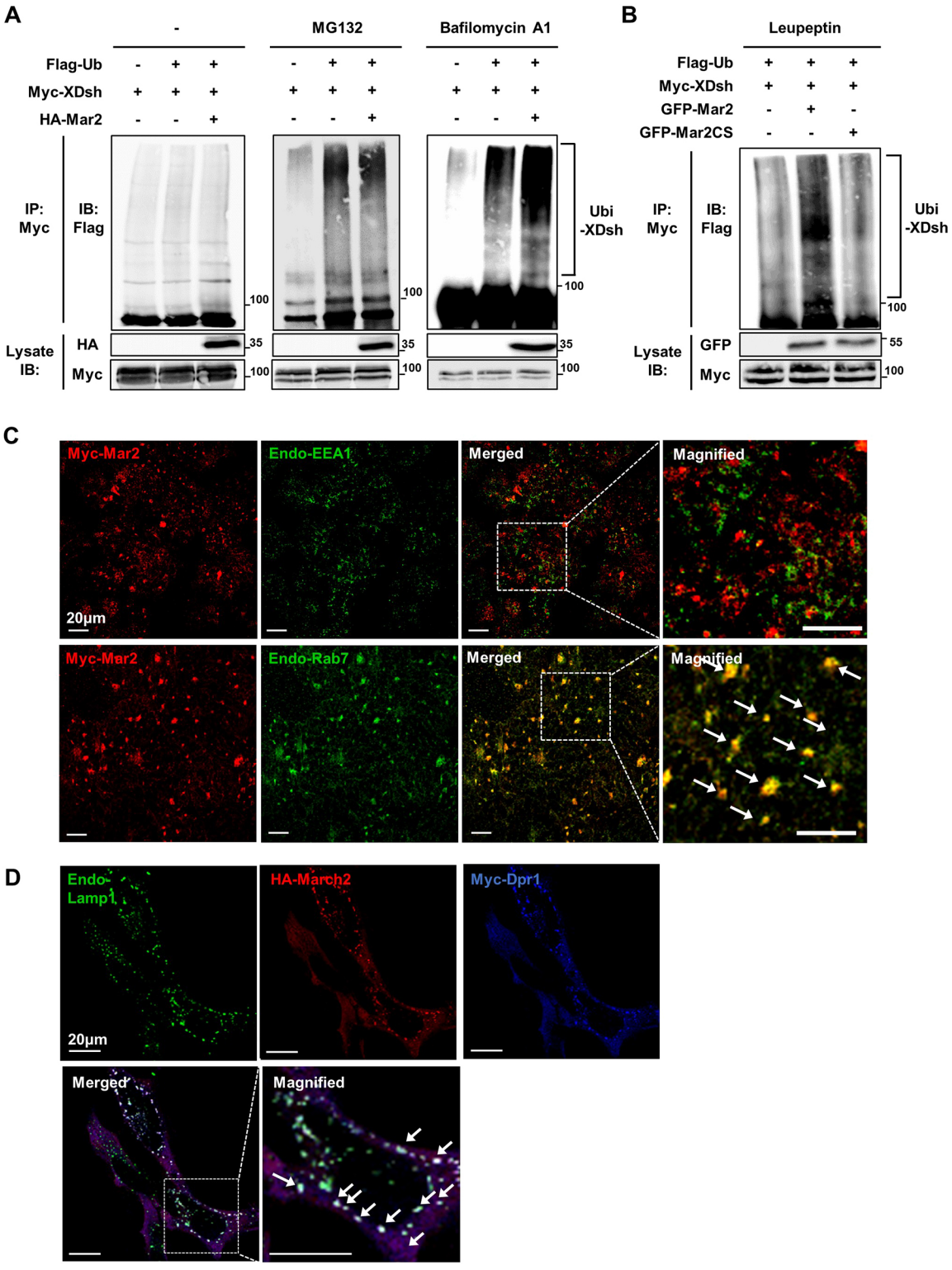

Fig. 3. March2 mediates Dsh for the lysosomal degradation pathway. (A,B) *In vivo* ubiquitylation assays in *Xenopus*. XDsh was pulled down with anti-Myc antibody and its ubiquitylation was detected by anti-Flag antibody. Poly-ubiquitylated Dsh protein was increased by March2 with bafilomycin A1 (A) or leupeptin (B) treatment. (C) Confocal images of *Xenopus* tissues showing the subcellular localization of March2 protein. Animal caps injected with Myc-Mar2 mRNA (200 pg) were immunostained with anti-EEA1 or Rab7 antibodies and analyzed. White arrows indicate colocalized puncta of March2 with Rab7. (D) Confocal images of HeLa cells showing colocalization of March2 and Dpr1 in Lamp1-positive puncta (white arrows).

overexpression of March2, but not March2CS, inhibited both Wnt8-mediated processes, confirming the idea that March2 acts as a negative regulator of canonical Wnt signaling (Fig. 4C, lanes 4-6).

We also tested whether the severity of phenotypes caused by forced Wnt signaling is increased by knockdown of March2. The ability of *Xenopus* embryos to form a secondary axis by Wnt8 in ventral regions was enhanced by March2 depletion (Fig. 4E). This

Development (2018) 145, dev143107. doi:10.1242/dev.143107

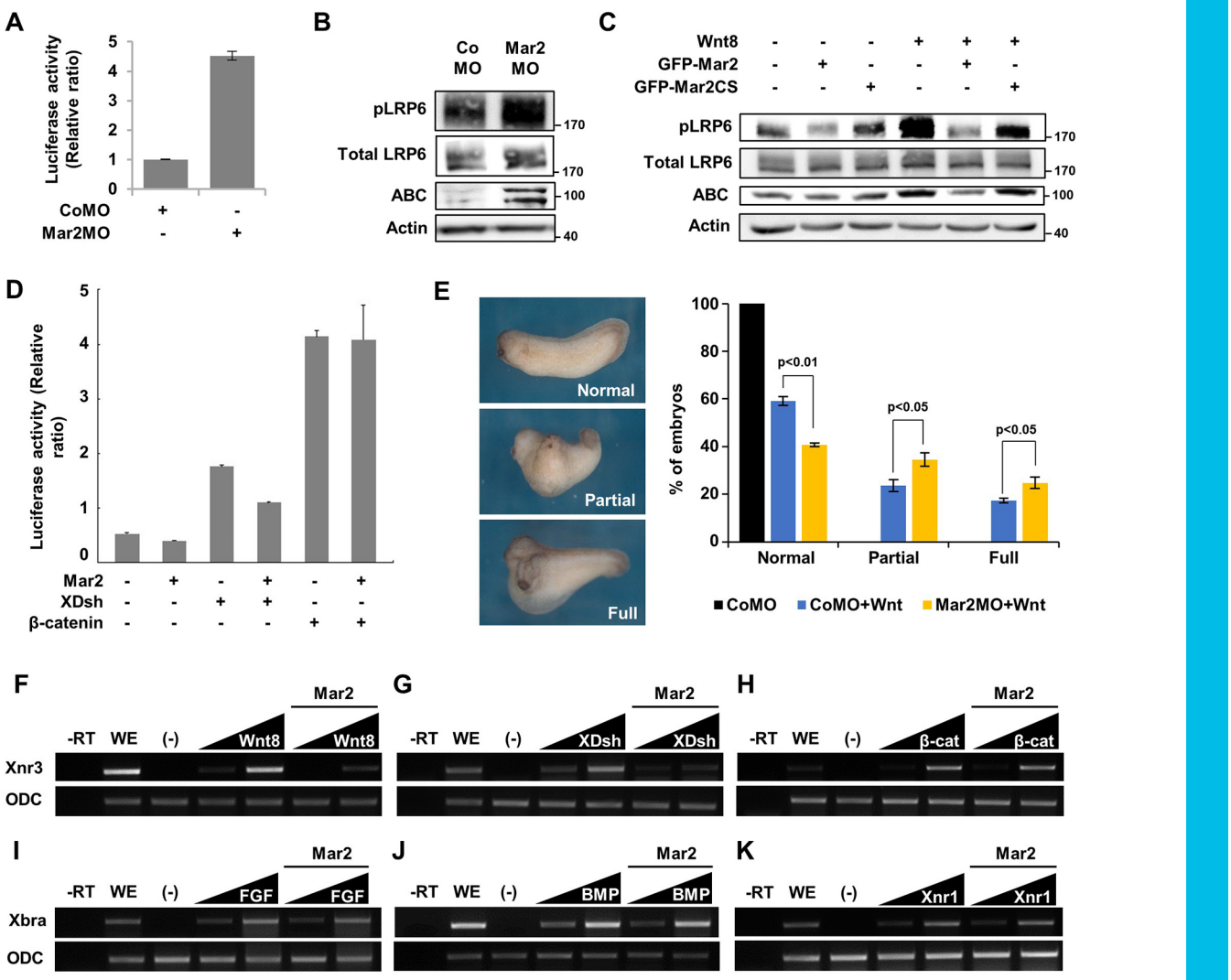

Fig. 4. March2 antagonizes canonical Wnt signaling in *Xenopus*. (A) Mar2MO (40 ng) increases TOPFlash activity in *Xenopus*. Error bars represent s.d. of triplicate experiments. *P*=0.0022. (B) Mar2MO mediates activation of β-catenin (ABC) and phosphorylation of LRP6. Four-cell stage embryos were dorsally injected with CoMO or Mar2MO (40 ng) and analyzed at stage 10.5. Actin and total LRP6: loading controls. (C) GFP-Mar2 mRNA (1 ng) expression but not GFP-Mar2CS mRNA (1 ng) decreases Wnt8 mRNA (20 pg)-mediated activation of β-catenin and phosphorylation of LRP6 in *Xenopus*. (D) Mar2 mRNA (1 ng) expression decreases TOPFlash activity induced by Dsh (2 ng) but not by β-catenin (200 pg). Error bars represent s.d. of triplicate experiments. (E) Mar2MO increases the severity of the Wnt8-induced ectopic axis. Wnt8 mRNA (1 pg) was injected with or without Mar2MO (50 ng) at the ventral side of the four-cell stage embryos and phenotypes were analyzed at the tadpole stage. 'Partial' indicates axis without head, including eyes and cement glands. 'Full' indicates axis with head. Statistical analysis was carried out on three independent experiments. Statistically significant differences between two sets are indicated. *P* values were obtained using two-tailed Student's *t*-test (see also Table S3). (F-H) RT-PCR analyses show that March2 inhibited Wnt8 or Dsh-induced *Xnr3* expression in *Xenopus* animal caps (F,G) but did not inhibit β-catenin-induced *Xnr3* expression (H). The amounts of injected mRNAs: Wnt8, 20 and 50 pg; XDsh, 1 and 2 ng; β-catenin, 50 and 100 pg; Mar2, 1 ng. (I-K) March2 did not inhibit FGF (I) and BMP (J); Nodal signals (K) mediated induction of *Xbra* expression. ODC serves as a loading control. -RT, control RT-PCR without reverse transcriptase; WE, whole embryos. Amounts of injected mRNAs: FGF, 50 and 150 pg; BMP, 50 and 200 pg; Xnr1, 100 and 200 pg; Mar2, 1 ng.

antagonistic role of March2 was specific for canonical Wnt signaling, because March2 inhibited Wnt- and Dsh-induced *Xnr3* expression (Fig. 4F,G), but did not affect FGF-, BMP- or nodal (Xnr1)-induced *Xbra* expression (Fig. 4I-K). Notably, March2 did not inhibit β-catenin-induced *Xnr3* expression, consistent with reporter assay results showing that March2 functions upstream of β-catenin (Fig. 4D,H).

March2 is required for anterior head formation

Our results clearly show that March2 antagonizes the canonical Wnt pathway by ubiquitylating Dsh protein and targeting it for lysosomal degradation. To elucidate the endogenous function of March2 in *Xenopus*, we injected Mar2MOs into the two dorsal blastomeres of four-to eight-cell stage embryos and analyzed their phenotypes at tadpole stages (Fig. 5A, Figs S6F and 7E). Intriguingly, almost 90% of March2 morphants exhibited defects in anterior head formation, including shrinkage or loss of forebrain structures, and in the cement gland and eyes, whereas embryos injected with control MO (CoMO) were normal. The phenotypes of March2 morphants were rescued by co-injection of the MOs-resistant form of mRNA or March2 DNA, confirming the specificity of the effects of the MOs (Fig. 5A,B, Fig. S6F,G, Fig. S7E,F). Meanwhile, gain-of-function of wild-type March2, but not March2CS, caused gastrulation defects (Fig. S3) that phenocopy of Dsh morphants (Sheng et al.,

Development (2018) 145, dev143107. doi:10.1242/dev.143107

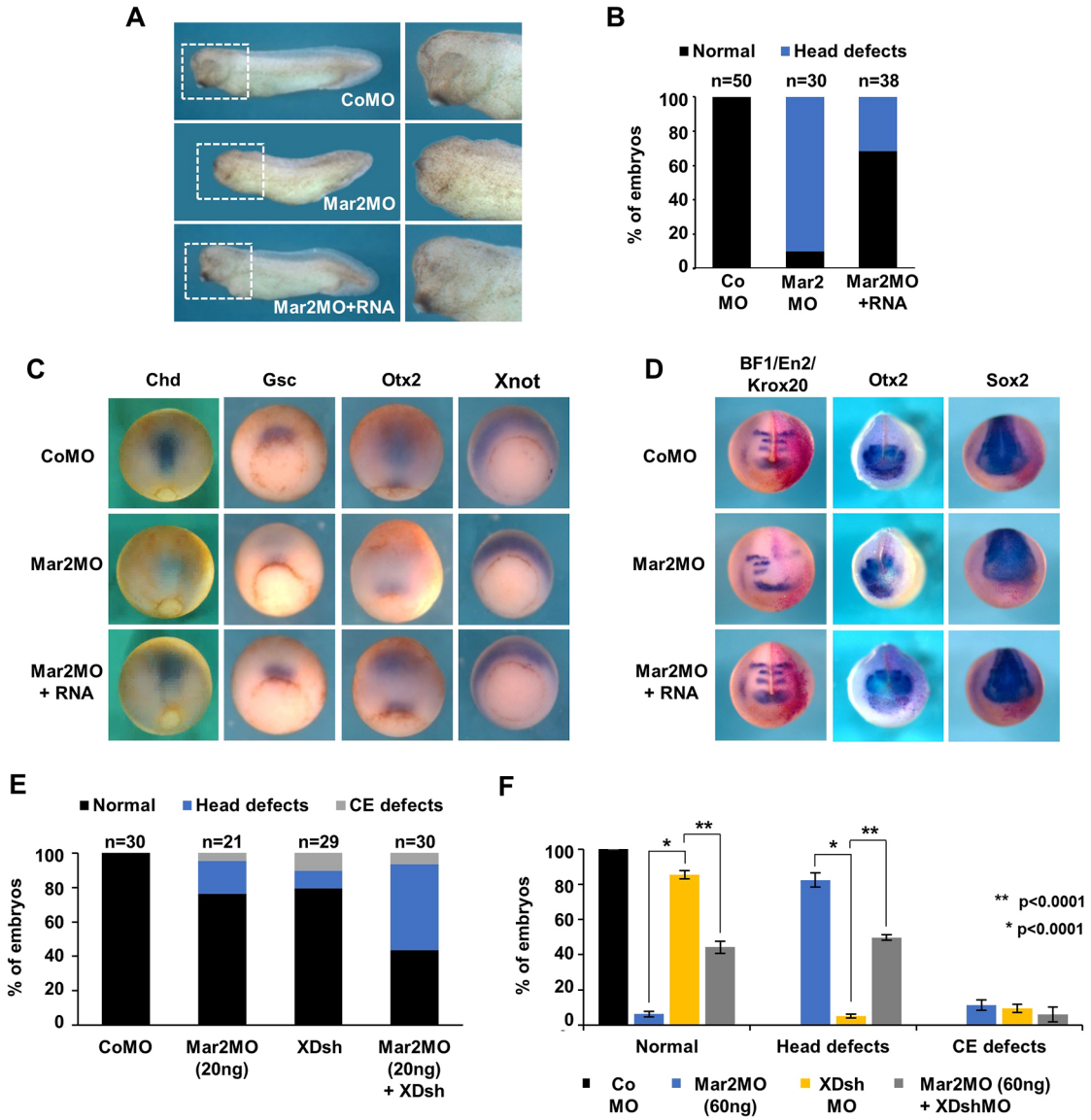

Fig. 5. March2 is required for anterior head formation in *Xenopus*. (A) Dorso-animal injection of Mar2MO (40 ng) at the eight-cell stage results in defects in anterior head formation; these defects were rescued by co-expression of a MO-resistant form of *Xenopus* March2 mRNA (500 pg). (B) Quantification of A. (C) *In situ* hybridization analysis showing that Mar2MO (40 ng) suppresses expression of *Chd* at stage 12, and *Gsc* and *Otx2* at stage 11.5. Co-expression of March2 mRNA (500 pg) rescues the reduction of expression of these genes (see Fig. S5A). (D) Mar2MO suppresses expression of *BF1*, *Otx2*, *En2* and *Krox20* at stage 17. CoMO (40 ng) or Mar2MO (40 ng) along with β-galactosidase mRNA (100 pg) as a lineage tracer were injected into one dorso-animal blastomere of eight-cell stage embryos. The right side of the embryos shown have been injected with indicated reagents (see Fig. S5B). (E,F) March2 regulates head formation through Dsh. Two dorsoanimal blastomeres of eight-cell stage embryos were injected with indicated reagents, and phenotypes were analyzed at tadpole stages. (E) Mar2MO (20 ng) along with Dsh mRNA (250 pg) synergistically induced head defects. (F) Head defects caused by Mar2MO (60 ng) were partially rescued by DshMO (40 ng). Statistical analysis was performed on three independent experiments. *P* values were obtained using two-tailed Student's *t*-test. For the number of embryos in each quantification, see Table S3.

2014), supporting our results suggesting that March2 downregulates the stability of Dsh protein (Fig. 2).

As March2 knockdown promotes excessive Wnt signaling by preserving the cytosolic pool of Dsh protein (Fig. 4), we asked whether the head defects caused by March2MO could be rescued by Axin1, an inhibitor of Wnt signaling that acts downstream of Dsh, and whether the head-enlargement defects caused by expression of Dkk1, a Wnt inhibitor upstream of Dsh, could be moderated by depletion of March2 (Fig. S4A,B). The head malformation caused by Mar2MO was significantly rescued by Axin1 (Fig. S4A,D), whereas that caused by Dkk1 was significantly rescued by Mar2MO (Fig. S4B). These results support the notion that the defects caused by March2 depletion are attributable to excessive Wnt signaling by stabilized Dsh protein.

Next, we asked whether March2 knockdown leads to impaired dorsal head organizer formation. Importantly, our results revealed that March2-depleted embryos showed decreased expression of the dorsal head organizer marker genes *Chd*, *Gsc* and *Otx2* at mid-to-late gastrula stages (st. 11-12), and these reductions were restored by expression of the MO-resistant form of March2 mRNA; in contrast, March2 depletion did not affect expression of the notochord marker *Xnot*, which is dispensable for head organizer formation (Fig. 5C and Figs S5A, S6H,I, S7G,H). Notably, prior to stage 11, Mar2MO did not inhibit expressions of *Gsc* and *Chd* (data not shown), which

Development (2018) 145, dev143107. doi:10.1242/dev.143107

are regulated by maternal Wnt signaling (Cho et al., 1991; Christian and Moon, 1993; Zhang et al., 2012). Moreover, March2 mRNA rescued head defects caused by Wnt8 DNA, which is capable of activating zygotic Wnt signaling (Fig. S4C). Collectively, these results suggest that March2 is required for head organizer formation by inhibiting zygotic Wnt signaling in *Xenopus*.

It has been reported that maintenance of the lowest levels of Wnt signaling at the head organizer during gastrulation results in precise anterior-posterior (AP) neural patterning by keeping anterior Wnt signaling low (De Robertis and Kuroda, 2004; Harland and Gerhart, 1997; Niehrs, 2004; Zhang et al., 2012). To further explore this concept, we next investigated the possibility that the effect of March2 depletion on the head organizer is translated into AP patterning. Injection of Mar2MO into one dorso-animal blastomere at the eight-cell stage reduced the expression of a subset of genes, including the forebrain markers *BF1* and *Otx2*, the midbrain marker *En2*, and the hindbrain marker *Krox20*; notably, these reductions were rescued by the MO-resistant form of March2 mRNA (Fig. 5D and Fig. S5B). Given that Wnt inhibition is also required for neural induction (Zhang et al., 2015), we examined the possibility that March2 may be involved in this process by analyzing the effects of March2 depletion on expression of the pan-neural marker *Sox2*. We found that Mar2MO did not affect *Sox2* expression, implying that March2 function is dispensable for neural induction (Fig. 5D). Interestingly, moderate depletion of endogenous March2 using a sub-optimal dose of Mar2MO that does not efficiently induce head defects, combined with a small increase in Dsh expression, synergistically induced head defects (Fig. 5E). This result can be interpreted to mean that the aberrant amount of Dsh protein arising from both Mar2MO-stabilized endogenous Dsh protein and ectopically expressed Dsh mRNA elevates Wnt signaling sufficiently to mediate head defects. Furthermore, the severity of head defects in March2 morphants caused by sufficient amounts of Mar2MO was ameliorated by moderate knockdown of Dsh with a sub-optimal dose of DshMO (Fig. 5F). These results imply that translation blockade of newly synthesized Dsh mRNA by DshMO counteracted the preservation of the existing pool of Dsh protein by Mar2MO (Fig. 5F), thereby rescuing the head defects in March2 morphants caused by the elevation in Wnt signaling attributable to increased Dsh protein. Collectively, these results underscore the requirement of March2 for anterior head formation through its Dsh-degradation-dependent antagonism of Wnt signaling.

Dpr1 is required for March2-mediated ubiquitylation and degradation of Dsh

As our *in situ* hybridization and RT-PCR results suggested the maternal and ubiquitous expression of *Xenopus* March2 transcripts during gastrulation (Fig. S1), we initially expected March2 to be involved in Wnt signaling in both dorsal and ventral regions of the embryo, and accordingly addressed the effects of March2 knockdown in each region. Intriguingly, however, Mar2MOs injection into the dorso-animal side caused head malformation, which is characteristic of genes that antagonize Wnt signaling (Fig. 5A, Figs S6F and S7E) (Shimomura et al., 2010; Zhang et al., 2012, 2015), whereas ventral injection did not cause any defects (data not shown). Consistent with this unanticipated physiological requirement, we found that March2 mediated degradation of Dsh protein in only dorsal and animal explants of the gastrula (stage 10.5) embryo (Fig. S8A). Notably, Dsh protein was stabilized to a greater extent in ventral explants.

These unexpected findings raise a question regarding how March2 specifically mediates degradation of Dsh protein in the dorso-animal region to promote precise head formation. One possible hypothesis is that an unidentified regulator of March2 that is enriched in the dorso-animal region ensures the region-specific function of March2. To test this idea, we postulated that the Dsh-interacting protein Dpr1/DACT1 is an unidentified regulator of March2, based on reports suggesting that: (1) Dpr1, which lacks enzymatic activity, interacts with PDZ and DEP domains of Dvl to mediate Dvl degradation via the lysosomal pathway (Kivimäe et al., 2011; Zhang et al., 2006); (2) Dpr1 transcripts are strongly expressed in the dorso-animal region of the *Xenopus* gastrula (Cheyette et al., 2002) (Fig. S8B); and (3) gain and loss of Dpr1 function phenocopy March2 gain and loss of function (Cheyette et al., 2002) (Fig. S3).

To corroborate the involvement of Dpr1 in March2 function in Wnt signaling and head formation, we first examined whether depletion of Dpr1 affected the ability of March2 to mediate Dsh degradation. Surprisingly, Dsh protein degradation induced by ectopically expressed March2 was attenuated by increasing amounts of co-injected Dpr1MO, which efficiently depleted Dpr1 protein expression in *Xenopus* (Fig. S8D), and additional co-injection of the MO-resistant form of Dpr1 mRNA restored the ability of March2 to degrade Dsh (Fig. 6A). Conversely, ectopically expressed Dpr1 decreased Dsh protein, and this effect was impaired by Mar2MOs and restored by co-injection of March2 mRNA (Fig. 6B and Fig. S6J). Moreover, March2 did not decrease Dsh protein when co-expressed with the dominant-negative form (DN) of Dpr1 (Zhang et al., 2006) (Fig. 6C). *In vivo* ubiquitylation assays showed that, in the presence of bafilomycin A1, Dpr1MO reduced March2-mediated poly-ubiquitylation of Dsh (Fig. 6D). Collectively, these results suggest that March2 requires Dpr1 to mediate poly-ubiquitylation and lysosomal degradation of Dsh, and further imply that the previously reported function of Dpr1 in promoting Dsh degradation (Zhang et al., 2006) depends on March2.

It is known that Dpr1 is a non-enzymatic Dsh-binding scaffold protein that lacks domains responsible for protein ubiquitylation and degradation. These observations, together with our findings, suggest that Dpr1 binds March2, serving as a bridge between March2 and Dsh to support the E3 ubiquitin ligase function of March2. To provide evidence supporting this hypothesis, we analyzed whether Dpr1 interacts with March2. Co-IP analyses showed that Dpr1 bound March2 (Fig. 6E). Consistent with this, confocal imaging (Figs 6F-J and 3D) showed that Dsh, Dpr1 and March2 proteins are co-localized in cytosolic vesicles (Fig. 6I,J) that our data suggest are late endosomes/lysosomes (Fig. 3C,D). Importantly, knockdown of Dpr1 both eliminated Dsh from lysosomes where March2 is localized (Fig. S9) and dramatically decreased the binding affinity of March2 for Dsh (Fig. 6K), suggesting that March2 requires Dpr1 to ensure stable interactions with Dsh in lysosomes and subsequent mediation of Dsh degradation.

Dpr1 is required for March2 to antagonize canonical Wnt signaling during anterior head formation

Next, we investigated whether March2 requires Dpr1 to antagonize the Wnt pathway in *Xenopus*. Our results showed that increasing amount of Dpr1MO impaired the ability of March2 to inhibit Wnt8-mediated β-catenin activation and LRP6 phosphorylation, whereas co-expression of Dpr1 mRNA restored the effects of March2 (Fig. 7A). Furthermore, co-expression of DN Dpr1 blocked the effect of March2 on Wnt8-mediated β-catenin activation (Fig. 7B), confirming our previous results showing that March2 is a negative regulator of the Wnt pathway and that Dpr1 is required for this process.

Development (2018) 145, dev143107. doi:10.1242/dev.143107

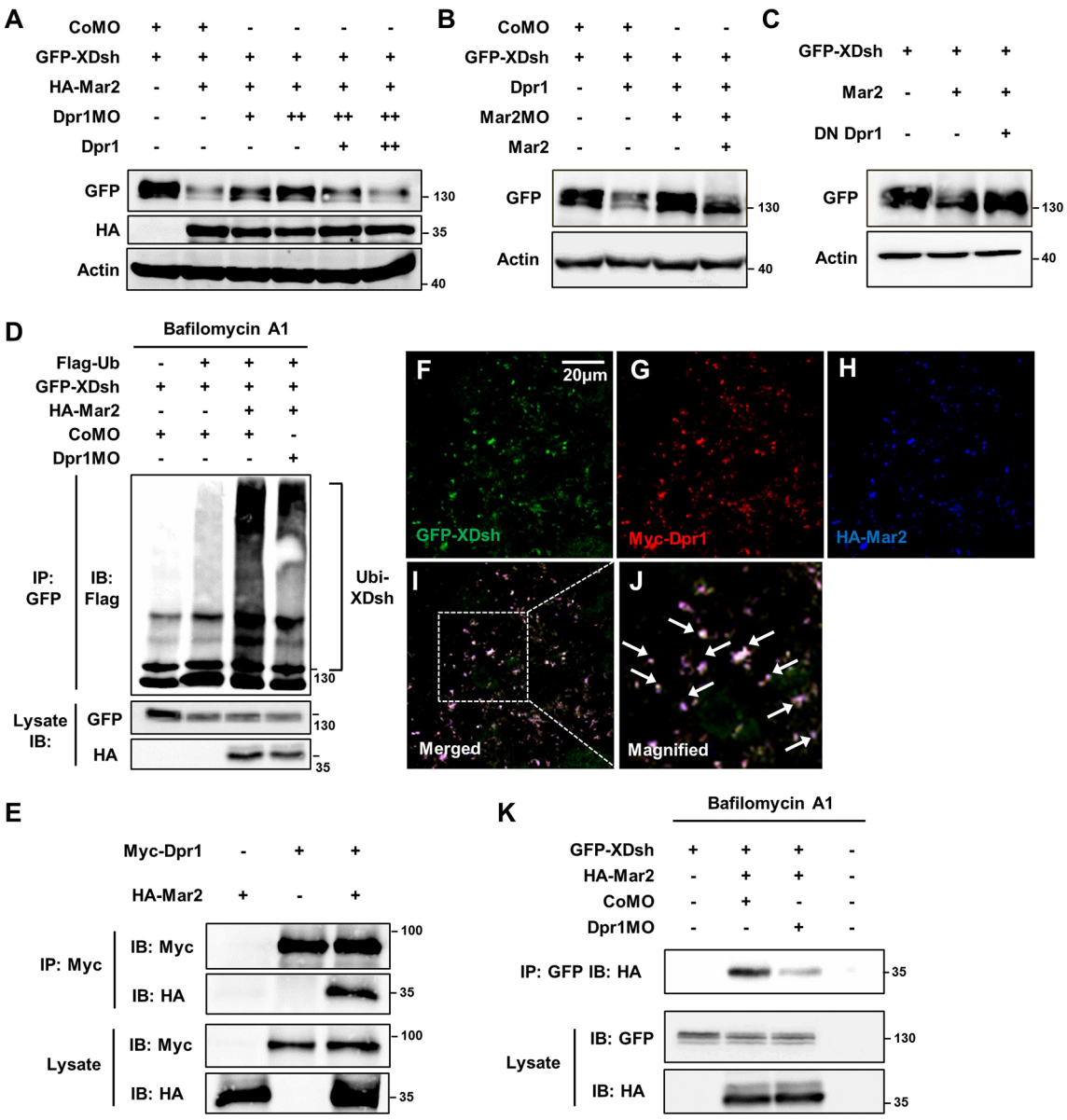

Fig. 6. March2 interacts with Dapper1 for Dsh degradation. (A) Dpr1MO impairs the March2-mediated decrease of Dsh protein. Four-cell stage embryos were dorso-animally injected with the indicated reagents and analyzed at stage 12. Amounts of injected mRNAs and MOs: GFP-XDsh, 200 pg; HA-Mar2, 1 ng; CoMO, 40 ng; Dpr1MO, 20 (+) and 40 ng (++); Dpr1, 1 (+) and 2 ng (++). (B) Mar2MO inhibits the Dpr1-mediated decrease in Dsh. Amounts of injected mRNAs and MOs: GFP-XDsh, 200 pg; Mar2, 1 ng; CoMO and Mar2MO, 40 ng; Dpr1, 2 ng. (C) The dominant-negative (DN) form of Dpr1 inhibits the March2-mediated decrease of Dsh. Amounts of injected mRNAs: GFP-Dsh, 200 pg; Mar2, 1 ng; DN Dpr1, 2 ng. (D) *In vivo* ubiquitylation assays showing that Dpr1MO (40 ng) reduces Mar2-mediated poly-ubiquitylation of Dsh. (E) Co-immunoprecipitation analysis showing that March2 binds Dpr1 in HEK293 T cells. (F-J) Dsh, Dpr1 and March2 are colocalized in *Xenopus*. Animal caps injected with GFP-XDsh (250 pg), Myc-Dpr1 (250 pg) and HA-Mar2 (250 pg) mRNAs were analyzed. White arrows (J) indicate Dsh-Dpr1-Mar2 colocalized puncta. (K) Co-immunoprecipitation analysis in *Xenopus* embryos showing Dpr1MO weakens the binding affinity between Mar2 and Dsh. Amounts of injected mRNAs and MOs: GFP-XDsh, 1 ng; HA-Mar2,1 ng; CoMO and Dpr1MO, 40 ng.

Last, we analyzed the involvement of Dpr1 in March2-mediated regulation of head formation. Consistent with our previous data (Fig. S4C), we found that ectopic expression of March2 efficiently suppressed the severity of head defects induced by Wnt8. However, co-injection of Dpr1MO abrogated this rescue effect of March2 (Fig. 7C). Furthermore, moderate depletion of both endogenous March2 and Dpr1 by injection of sub-optimal doses of MOs synergistically induced head defects (Fig. 7D). This result can be interpreted as indicating that the combination of moderate blockade of endogenous March2 mRNA translation by Mar2MO and inhibition of endogenous March2 protein function by depletion of Dpr1 causes a degree of March2 malfunction sufficient to stabilize aberrant amounts of Dsh protein and cause head defects.

DISCUSSION

This study reveals a previously unknown function of March2 during head formation in *Xenopus*. March proteins are recently identified members of the mammalian E3 ubiquitin ligase family. Compared with other classes of E3 ubiquitin ligases, evidence relating to the roles of March family proteins *in vivo* or *in vitro* is limited. A few studies in cultured cells have reported functions of March family proteins in keeping with a role in endosomal

Development (2018) 145, dev143107. doi:10.1242/dev.143107

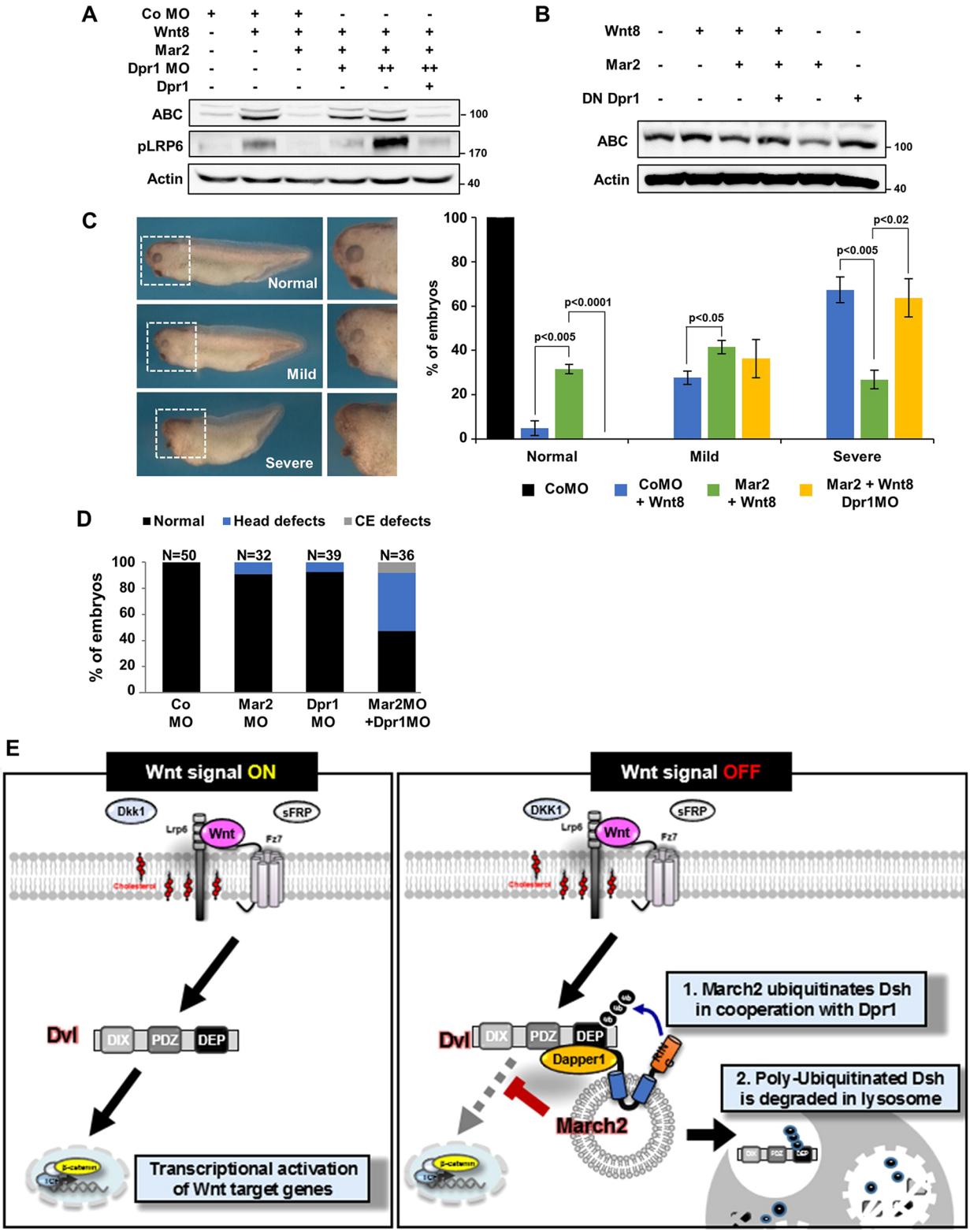

Fig. 7. March2 antagonizes canonical Wnt signaling in concert with Dapper1 for head formation. (A) Dpr1MO impairs the March2-mediated decrease of activated β-catenin and phosphorylated LRP6 levels. Amounts of injected mRNAs and MOs: Wnt8, 20 pg; March2, 1 ng; CoMO, 40 ng; Dpr1MO, 20 and 40 ng, respectively; Dpr1, 1 ng. (B) DN Dpr1 mRNA (2 ng) impedes the March2 mRNA (1 ng)-mediated decrease of activated β-catenin. (C) Rescuing ability of March2 mRNA (1 ng) for the Wnt8 DNA (40 pg)-mediated head defect was impeded by Dpr1MO (40 ng). 'Severe' denotes eyeless, malformation of cement glands and loss of anterior head structures. 'Mild' denotes small sizes of eyes and head. Statistical analysis was carried out on three independent experiments. *P* values were obtained using two-tailed Student's *t*-test (see also Table S3). (D) Malfunction of endogenous March2 by moderate doses of Mar2MO (20 ng) and Dpr1MO (20 ng) induced head defects (see also Table S3). (E) Model for March2-mediated Dsh degradation in *Xenopus*. Upon Wnt stimulation, Dsh relays signal for downstream gene transcription. To maintain the Wnt-off state, reduction of the cytosolic pool of Dsh is required. For this purpose, March2 binds and ubiquitylates Dsh in concert with Dpr1 for lysosomal degradation.

Development (2018) 145, dev143107. doi:10.1242/dev.143107

trafficking and lysosomal sorting of target proteins (Cao et al., 2008; Han et al., 2012; Nakamura et al., 2005). To date, however, the physiological functions of March family proteins have yet to be elucidated.

We investigated regulatory mechanisms of March2 that underlie head formation, and found that March2 acts as a negative regulator of canonical Wnt signaling by promoting the lysosomal degradation of Dsh. We showed that March2 is maternally and ubiquitously expressed throughout *Xenopus* embryogenesis, but is notable for its expression during gastrulation in the dorsal organizer and at neurula stages in anterior neural plate regions, which are responsible for head formation and are sites where Wnt signaling is actively antagonized (Figs S1 and S8). Of note, the March2 expression pattern is similar to that of Dsh in *Xenopus* gastrula (Gray et al., 2009), supporting our data suggesting that March2 targets Dsh for degradation in the dorsal head organizer to regulate precise head formation.

As first suggested by a bioinformatics analysis and further corroborated by biochemical analyses, our results clearly showed that *Xenopus* March2 is a novel Dsh-binding protein (Fig. 1). Using co-IP analyses with deletion-mutant forms of Dsh and March2, we further elucidated the mode of interaction between them. Intriguingly, we found that the C-terminal region of March2 interacts with PDZ and DEP domains of Dsh, and further showed that the conserved PDZ-binding motif at the tip of the March2 C terminus is dispensable for the interaction. Further examination to narrow down the specific amino acids of the C-terminal region of March2 will resolve this inconsistency.

According to the recently proposed model of canonical Wnt signaling, in the absence of Wnt stimulation, Dsh protein is located cytoplasmically (Barker and Clevers, 2006; Clevers, 2006; Gao and Chen, 2010). Wnt stimulation recruits Dsh to the Fz receptor in the cell membrane, where it functions as a scaffolding protein that serves to release β-catenin from the destruction complex by conveying it to the membrane. It has been reported that March2 is localized in the endoplasmic reticulum (ER), early and late endosomes, lysosome, multivesicular bodies (MVB), and Golgi structure (Han et al., 2012; Nakamura et al., 2005). However, our confocal images revealed that most March2 protein is localized to Rab7-positive late endosomes/lysosomes in *Xenopus* (Fig. 3C). Our results, taken together with the domain structure of March2, suggest that both the N terminus containing the RING domain and C-terminal region responsible for Dsh interaction may be exposed to the cytosol. From this vantage point, March2 captures excess cytosolic Dsh and clears it. This notion is distinguishable from the report demonstrating that Wnt activation sequesters negative regulators of Wnt signaling into the multivesicular endosomes (Taelman et al., 2010), because our examination showed that Wnt stimulation did not affect the ability of March2 to produce Dsh degradation (data not shown).

March2 acts through the mode of interaction described above to mediate poly-ubiquitylation and proteolysis of Dsh in *Xenopus* (Fig. 2). In fact, several E3 ubiquitin ligases and components that are responsible for Dsh degradation have been extensively investigated. These studies have revealed that Dsh protein turnover is regulated by NEDL-1, the KLHL12-Cullin-3 ubiquitin ligase complex, Prickle-1, ANAPC2 and NEDD4L (Angers et al., 2006; Chan et al., 2006; Ganner et al., 2009; Miyazaki et al., 2004; Zhang et al., 2014). Two novel aspects of March2-mediated Dsh degradation differentiate our study from these previous reports. First, we found that March2 is a novel E3-ubiquitin ligase that specifically regulates head formation via Dsh degradation to antagonize canonical Wnt signaling. It is well known that Dsh is a common denominator in both the canonical Wnt and the non-canonical Wnt/PCP pathway. Each pathway governs different processes in *Xenopus*. Canonical Wnt signaling is crucial for head formation, but non-canonical Wnt signaling is required for convergent extension (CE) movements. It has been suggested that ANAPC2 plays a central role in regulating cilia polarity in *Xenopus* epidermis via mediating Dsh degradation (Ganner et al., 2009). More recently, NEDD4L has also been suggested to be a Dsh-specific E3 ligase that mediates Dsh degradation and is required for CE movements (Zhang et al., 2014). Both reports described them as non-canonical Wnt signaling antagonists. Intriguingly, however, although March2 mediates degradation of Dsh, which serves as a branch point in both pathways, and March2 transcripts are also expressed in the region that undergoes CE movements, our results showed that March2 morphants only resulted in head defects that are specifically induced by excessive canonical Wnt signaling (Figs 4 and 5). They were unable to induce defective gastrulation (data not shown), which is a hallmark of mis-regulated non-canonical Wnt signaling. We suggest two regulatory mechanisms that allow Dsh to undergo canonical Wnt-specific degradation by March2: unknown components that help Dsh avoid capture by March2 in the lysosome under non-canonical Wnt stimulation; and the marking of Dsh with canonical Wnt-specific modification(s), such as phosphorylation, required for recognition by March2. Indeed, the latter idea is supported by data shown in Fig. 6B,C. We found that March2 expression significantly degraded the phosphorylated form of Dsh, which is lower in electrophoretic mobility. Although these ideas require more experimental evidence from further study, our study is the first to provide evidence of an E3 ubiquitin ligase for Dsh degradation that exerts roles in the vertebrate head formation. Furthermore, we suggest March2 as being the first identified E3 ubiquitin ligase responsible for lysosomal degradation of Dsh (Fig. 3). Although previous studies have reported that Dsh undergoes lysosomal degradation, the E3 ubiquitin ligase responsible for this pathway has remained unidentified. The Dsh-interacting protein Dpr1, though not itself an E3 ubiquitin ligase, was the only well-identified protein implicated in lysosome-dependent Dsh degradation, as evidenced by the ability of lysosomal inhibitors to recover the Dpr1-mediated reduction in Dsh protein. We thus posit March2 as a genuine ubiquitin ligase that requires Dpr1 for Dsh degradation. Indeed, our results confirm that Dpr1 aids March2-mediated degradation of Dsh by allowing stable, strong interactions between March2 and Dsh through its scaffolding function, thereby producing the antagonism of the canonical Wnt signaling necessary for head formation (Figs 6 and 7 and Fig. S8). Moreover, these results explain how ubiquitously expressed March2 can mediate the specific degradation of Dsh protein at the dorso-animal region, which is needed for precise head formation. It is still not known how Dpr1 and March2 effectively cooperate to target Dsh for degradation in the lysosomes – a mechanism that awaits further study.

On the basis of our results, we propose the following model in which March2 in the dorsal head organizer antagonizes canonical Wnt signaling by targeting Dsh for lysosomal degradation (Fig. 7E): (1) cytosolic vesicle-localized March2 binds through its C-terminal region to DEP and PDZ domains of Dsh in concert with Dpr1, which acts via its scaffolding function to ensure stable interactions between March2 and Dsh; (2) March2 mediates the poly-ubiquitylation of Dsh, and targets Dsh to the lysosomal degradation pathway; and (3) the reduced pool of Dsh protein in the cytosol ensures the turned-off status of Wnt signaling, which is necessary for head formation. Further studies will be required to elucidate in detail how Dpr1 is involved in

Development (2018) 145, dev143107. doi:10.1242/dev.143107

the mechanism by which March2 regulates Dsh degradation during head formation. Nevertheless, the present study provides new insights into the mechanisms that regulate the canonical Wnt pathway as well as the process of head formation during vertebrate development.

MATERIALS AND METHODS

Bioinformatics analysis

To perform a computational screening analysis, we predicted the ligand selectivity of the PDZ domain of *Xenopus* Dsh with the PDZ domain specificity prediction tool (http://sbi.postech.ac.kr/pdz/) and scored potential binding partners of *Xenopus* proteins. The prediction tool first selects pocket residues of PDZ domain from the query sequence with sequence alignment for the reference PDZ domain. Then, it predicts pocket-wise ligand selectivity as a positional weight matrix (PWM) based on the pocket residue similarity with those of a reference set of 133 PDZ domains using the 10 physicochemical properties of amino acids, i.e. hydrogen bond donors, polarity, volume, bulkiness, hydrophobicity, isoelectric point, positive charge, negative charge, electron ion interaction potential and free energy in water. Finally the PWM allows us to calculate binding scores between candidate proteins and PDZ domain of query protein and to prioritize them.

Plasmids and mRNA synthesis

For expression in *Xenopus* embryos, the entire coding region of *Xenopus* March2 was amplified from gastrula-stage embryos by PCR and cloned into the pCS2+, pCS2+GFP and the pCS4+HA vectors, respectively. Deletion mutants of March2 (Mar2N and Mar2C) were generated with fusion PCR and cloned into the pCS2+GFP vector. For *Xenopus* March2CS, the 64th, 67th, 106th and 109th Cys residues were mutated into Ser residues using PCR-based mutagenesis. The entire coding region of *Xenopus* Dapper1 was also amplified from gastrula stage embryos by PCR and cloned into the pCST+ and pCS2+-Myc vectors. Capped mRNAs were synthesized from *Not*I-linearized plasmids using the SP6 mMessage mMachine kit (Ambion).

Cell culture and transfection

HEK293FT, HEK293T, HeLa cells were obtained from ATCC and maintained with Dulbecco's modified Eagle's medium (DMEM; Hyclone) containing 10% FBS and 1% antibiotics. Lipofectamine 2000 (Invitrogen) or Vivamagic transfection reagent (Vivagen) was used for cell transfections. All cells were maintained and transfected without any contamination.

Semi-quantitative RT-PCR

RT-PCR analysis was performed as described previously (Cheong et al., 2006). Primers for RT-PCR analysis were as follows: *March2* forward, 5′-ATGGCTTAAGGACCCAGGAC-3′; *March2* reverse, 5′-AGTGGTAGCGGAATGACACC-3′; *Dsh* forward, 5′-ATGGCGGAGACTAAAGTGATTTA-3′; *Dsh* reverse, 5′-TTCAGGTCTGACCTCTGTAG-3′; *Dpr1* forward, 5′-AGAGCATCTGGAGACAGAC-3′; *Dpr1* reverse, 5′-TGTAGTCCAGCCATTCAAGA-3′. Primers for *ODC*, *Xnr3*, *Siamois*, *Xbra*, *Msx1* and *Chordin* are listed in Table S4. Relative expression levels for Fig. S6B were analyzed using ImageJ.

Xenopus embryos and microinjection

Xenopus laevis females and males were purchased from Nasco and were used following the instructions from the POSTECH IACUC (Institutional Animal Care and Use Committees) (Korea) after they had certified us regarding ethical handling. *Xenopus laevis* eggs were obtained and fertilized as described previously (Sheng et al., 2014). Developmental stages of the embryos were determined according to Nieuwkoop and Faber (1994). Microinjections were performed as described previously (Sheng et al., 2014).

Antisense morpholino oligonucleotides

Antisense morpholino oligonucleotides (MO) were obtained from Gene Tools. MO sequences were as follows: March2 MO, 5′-TCATGGCAACCCTCAGTGCCTTCCT-3′; March2 MO2, 5′-CAACCCTCAGTGCCTTCCTCCTTTA-3′; March2 MO3, 5′-TGACTCTCCGCTGCCAGACTTTAC-3′; Dapper1 MO, 5′-GATCGGCTTCATCCTCTGGGAACGA-3′; XDsh MO, 5′-TCACTTTAGTCTCCGCCATTCTGCG-3′; control MO, 5′-CCTCTTACCTCAGTTACAATTTATA-3′.

Immunofluorescence

Two- to four-cell stage embryos were injected into the animal pole with mRNAs. At stage 9.5, animal caps were dissected, fixed in 4% paraformaldehyde for 2 h and incubated in PBS with 0.1% Triton X-100 and 2% BSA for 1 h. The tissues were stained with primary antibodies (listed in Table S1) for 2 h, washed with PBS and incubated with fluorescent secondary antibodies for 2 h at room temperature. Mounted tissue images were obtained and analyzed by confocal microscopy (Olympus FluoView 1000 and Zeiss LSM 510).

In vivo ubiquitylation assay

Injected stage 8 embryos were treated with 40 µM MG132, 250 µM bafilomycin A1 or 100 µM leupeptin and were harvested at stage 12. Embryos were lysed in RIPA buffer, and then pull-down steps and SDS-PAGE were performed.

In situ hybridization

Whole-mount *in situ* hybridization was performed as previously described (Harland, 1991). Antisense *in situ* probes against *March2* was generated by linearizing the pBSKII+March2 with *Bst*XI and transcribing with T7 RNA polymerase.

Acknowledgements

We thank Drs R. Moon, C. Niehrs, E. Jho, C. Yeo and S. Hirose for generous gifts of reagents. We also appreciate other members of our laboratory for helpful comments.

Competing interests

The authors declare no competing or financial interests.

Author contributions

Conceptualization: H.L., S.-M.C., J.-K.H.; Methodology: H.L., S.-M.C., S.-B.J., G.-S.C.; Software: J.-S.Y., S.K.; Validation: H.L., G.-S.C., J.-S.Y., S.K.; Formal analysis: H.L., S.-M.C., W.H., Y.K.; Investigation: H.L., S.-M.C., W.H., Y.K., S.-B.J., G.-S.C.; Resources: J.-S.Y.; Writing - original draft: H.L., S.-M.C., J.-K.H.; Writing - review & editing: H.L., S.-M.C., W.H., J.-K.H.; Visualization: H.L.; Supervision: J.-K.H.; Project administration: J.-K.H.; Funding acquisition: J.-K.H.

Funding

This work was supported by the National Research Foundation of Korea (NRF) grant funded by the Korea government (MSIP) (NRF-2017R1A2B2006101) and the BK21 PLUS Research Fellowship from the Ministry of Education, Science and Technology, Republic of Korea.

Supplementary information

Supplementary information available online at
http://dev.biologists.org/lookup/doi/10.1242/dev.143107.supplemental

References

Angers, S., Thorpe, C. J., Biechele, T. L., Goldenberg, S. J., Zheng, N., MacCoss, M. J. and Moon, R. T. (2006). The KLHL12-Cullin-3 ubiquitin ligase negatively regulates the Wnt-beta-catenin pathway by targeting Dishevelled for degradation. *Nat. Cell Biol.* **8**, 348-357.

Barker, N. and Clevers, H. (2006). Mining the Wnt pathway for cancer therapeutics. *Nat. Rev. Drug Discov.* **5**, 997-1014.

Bartee, E., Mansouri, M., Hovey Nerenberg, B. T., Gouveia, K. and Fruh, K. (2004). Downregulation of major histocompatibility complex class I by human ubiquitin ligases related to viral immune evasion proteins. *J. Virol.* **78**, 1109-1120.

Bilic, J., Huang, Y. L., Davidson, G., Zimmermann, T., Cruciat, C. M., Bienz, M. and Niehrs, C. (2007). Wnt induces LRP6 signalosomes and promotes dishevelled-dependent LRP6 phosphorylation. *Science* **316**, 1619-1622.

Cao, Z., Huett, A., Kuballa, P., Giallourakis, C. and Xavier, R. J. (2008). DLG1 is an anchor for the E3 ligase MARCH2 at sites of cell-cell contact. *Cell. Signal.* **20**, 73-82.

Chan, D. W., Chan, C. Y., Yam, J. W., Ching, Y. P. and Ng, I. O. (2006). Prickle-1 negatively regulates Wnt/beta-catenin pathway by promoting Dishevelled ubiquitination/degradation in liver cancer. *Gastroenterology* **131**, 1218-1227.

Cheng, J. and Guggino, W. (2013). Ubiquitination and degradation of CFTR by the E3 ubiquitin ligase MARCH2 through its association with adaptor proteins CAL and STX6. *PLoS ONE* **8**, e68001.
Cheong, S.-M., Choi, S.-C. and Han, J.-K. (2006). Xenopus Dab2 is required for embryonic angiogenesis. *BMC Dev. Biol.* **6**, 63.
Cheyette, B. N., Waxman, J. S., Miller, J. R., Takemaru, K., Sheldahl, L. C., Khlebtsova, N., Fox, E. P., Earnest, T. and Moon, R. T. (2002). Dapper, a Dishevelled-associated antagonist of beta-catenin and JNK signaling, is required for notochord formation. *Dev. Cell* **2**, 449-461.
Cho, K. W., Blumberg, B., Steinbeisser, H. and De Robertis, E. M. (1991). Molecular nature of Spemann's organizer: the role of the Xenopus homeobox gene goosecoid. *Cell* **67**, 1111-1120.
Christian, J. L. and Moon, R. T. (1993). Interactions between Xwnt-8 and Spemann organizer signaling pathways generate dorsoventral pattern in the embryonic mesoderm of Xenopus. *Genes Dev.* **7**, 13-28.
Clevers, H. (2006). Wnt/beta-catenin signaling in development and disease. *Cell* **127**, 469-480.
De Robertis, E. M. and and Kuroda, H. (2004). Dorsal-ventral patterning and neural induction in Xenopus embryos. *Annu. Rev. Cell Dev. Biol.* **20**, 285-308.
Ganner, A., Lienkamp, S., Schafer, T., Romaker, D., Wegierski, T., Park, T. J., Spreitzer, S., Simons, M., Gloy, J., Kim, E. et al. (2009). Regulation of ciliary polarity by the APC/C. *Proc. Natl. Acad. Sci. USA* **106**, 17799-17804.
Gao, C. and Chen, Y. G. (2010). Dishevelled: the hub of Wnt signaling. *Cell. Signal.* **22**, 717-727.
Gao, C., Cao, W., Bao, L., Zuo, W., Xie, G., Cai, T., Fu, W., Zhang, J., Wu, W., Zhang, X. et al. (2010). Autophagy negatively regulates Wnt signalling by promoting Dishevelled degradation. *Nat. Cell Biol.* **12**, 781-790.
Glinka, A., Wu, W., Onichtchouk, D., Blumenstock, C. and Niehrs, C. (1997). Head induction by simultaneous repression of Bmp and Wnt signalling in Xenopus. *Nature* **389**, 517-519.
Gray, R. S., Bayly, R. D., Green, S. A., Agarwala, S., Lowe, C. J. and Wallingford, J. B. (2009). Diversification of the expression patterns and developmental functions of the dishevelled gene family during chordate evolution. *Dev. Dyn.* **238**, 2044-2057.
Han, S. O., Xiao, K., Kim, J., Wu, J. H., Wisler, J. W., Nakamura, N., Freedman, N. J. and Shenoy, S. K. (2012). MARCH2 promotes endocytosis and lysosomal sorting of carvedilol-bound beta(2)-adrenergic receptors. *J. Cell Biol.* **199**, 817-830.
Harland, R. M. (1991). In situ hybridization: an improved whole-mount method for Xenopus embryos. *Methods Cell Biol.* **36**, 685-695.
Harland, R. and Gerhart, J. (1997). Formation and function of Spemann's organizer. *Annu. Rev. Cell Dev. Biol.* **13**, 611-667.
Kiecker, C. and Niehrs, C. (2001). A morphogen gradient of Wnt/beta-catenin signalling regulates anteroposterior neural patterning in Xenopus. *Development* **128**, 4189-4201.
Kim, J., Kim, I., Yang, J.-S., Shin, Y.-E., Hwang, J., Park, S., Choi, Y. S. and Kim, S. (2012). Rewiring of PDZ domain-ligand interaction network contributed to eukaryotic evolution. *PLoS Genet.* **8**, e1002510.
Kivimäe, S., Yang, X. Y. and Cheyette, B. N. (2011). All Dact (Dapper/Frodo) scaffold proteins dimerize and exhibit conserved interactions with Vangl, Dvl, and serine/threonine kinases. *BMC Biochem.* **12**, 33.
Logan, C. Y. and Nusse, R. (2004). The Wnt signaling pathway in development and disease. *Annu. Rev. Cell Dev. Biol.* **20**, 781-810.
MacDonald, B. T., Tamai, K. and He, X. (2009). Wnt/beta-catenin signaling: components, mechanisms, and diseases. *Dev. Cell* **17**, 9-26.
Miyazaki, K., Fujita, T., Ozaki, T., Kato, C., Kurose, Y., Sakamoto, M., Kato, S., Goto, T., Itoyama, Y., Aoki, M. et al. (2004). NEDL1, a novel ubiquitin-protein isopeptide ligase for dishevelled-1, targets mutant superoxide dismutase-1. *J. Biol. Chem.* **279**, 11327-11335.
Nakamura, N., Fukuda, H., Kato, A. and Hirose, S. (2005). MARCH-II is a syntaxin-6-binding protein involved in endosomal trafficking. *Mol. Biol. Cell* **16**, 1696-1710.
Nieuwkoop, P. D. and Faber, J. (eds) (1994). *Normal Table of Xenopus laevis (Daudin)*. New York: Garland Publishing.
Niehrs, C. (2004). Regionally specific induction by the Spemann-Mangold organizer. *Nat. Rev. Genet.* **5**, 425-434.
Sheng, R., Kim, H., Lee, H., Xin, Y., Chen, Y., Tian, W., Cui, Y., Choi, J. C., Doh, J., Han, J. K. et al. (2014). Cholesterol selectively activates canonical Wnt signalling over non-canonical Wnt signalling. *Nat. Commun.* **5**, 4393.
Shimomura, Y., Agalliu, D., Vonica, A., Luria, V., Wajid, M., Baumer, A., Belli, S., Petukhova, L., Schinzel, A., Brivanlou, A. H. et al. (2010). APCDD1 is a novel Wnt inhibitor mutated in hereditary hypotrichosis simplex. *Nature* **464**, 1043-1047.
Taelman, V. F., Dobrowolski, R., Plouhinec, J. L., Fuentealba, L. C., Vorwald, P. P., Gumper, I., Sabatini, D. D. and De Robertis, E. M. (2010). Wnt signaling requires sequestration of glycogen synthase kinase 3 inside multivesicular endosomes. *Cell* **143**, 1136-1148.
Yamaguchi, T. P. (2001). Heads or tails: Wnts and anterior-posterior patterning. *Curr. Biol.* **11**, R713-R724.
Zhang, L., Gao, X., Wen, J., Ning, Y. and Chen, Y. G. (2006). Dapper 1 antagonizes Wnt signaling by promoting dishevelled degradation. *J. Biol. Chem.* **281**, 8607-8612.
Zhang, X., Abreu, J. G., Yokota, C., MacDonald, B. T., Singh, S., Coburn, K. L., Cheong, S. M., Zhang, M. M., Ye, Q. Z., Hang, H. C. et al. (2012). Tiki1 is required for head formation via Wnt cleavage-oxidation and inactivation. *Cell* **149**, 1565-1577.
Zhang, Y., Ding, Y., Chen, Y. G. and Tao, Q. (2014). NEDD4L regulates convergent extension movements in Xenopus embryos via Disheveled-mediated non-canonical Wnt signaling. *Dev. Biol.* **392**, 15-25.
Zhang, X., Cheong, S. M., Amado, N. G., Reis, A. H., MacDonald, B. T., Zebisch, M., Jones, E. Y., Abreu, J. G. and He, X. (2015). Notum is required for neural and head induction via Wnt deacylation, oxidation, and inactivation. *Dev. Cell* **32**, 719-730.

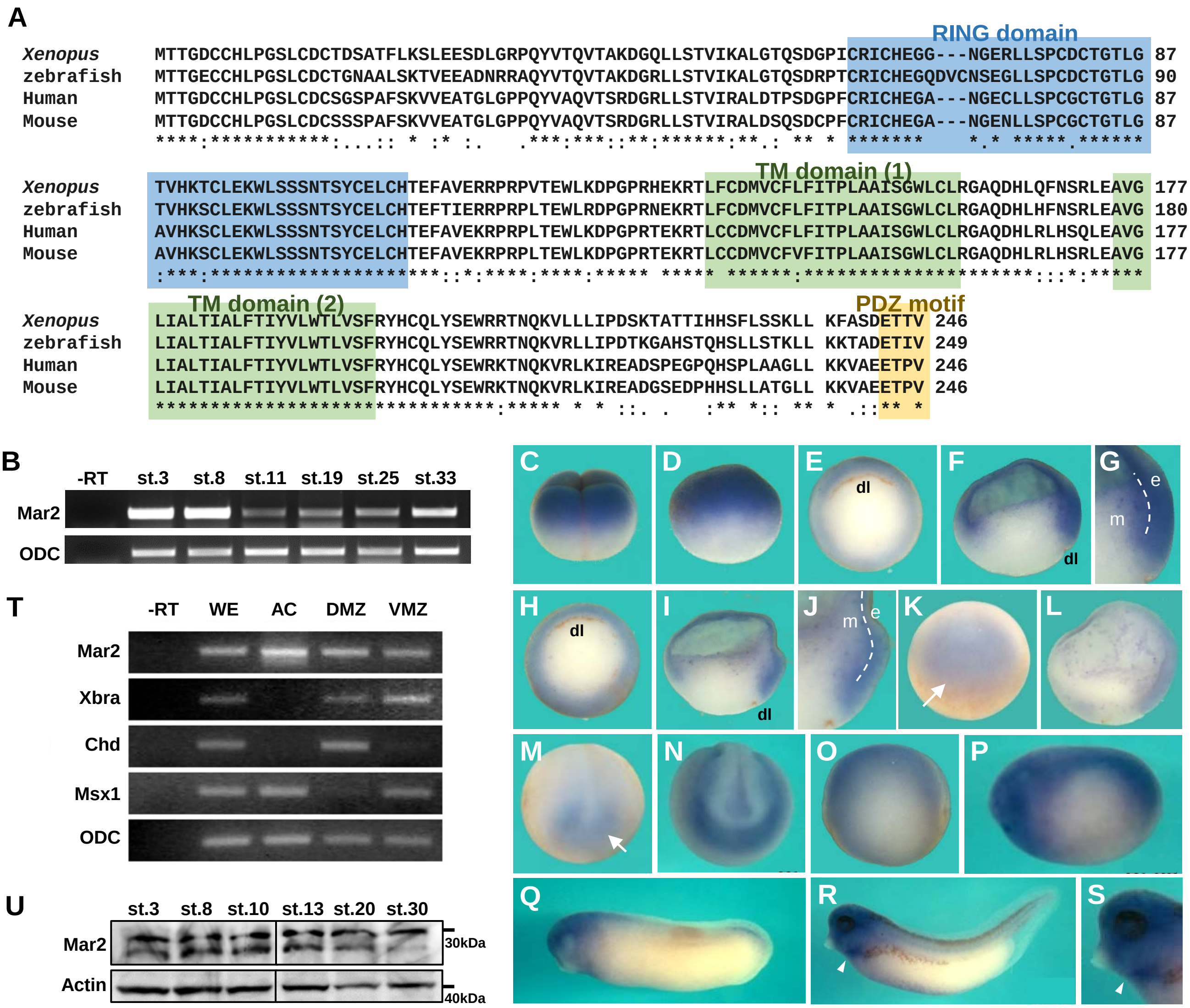

Fig. S1. Expression patterns of March2 transcripts and protein during *Xenopus* development (A) Amino acid sequence comparison among *Xenopus*, zebrafish, human and mouse March2. RING domain, two transmembrane (TM) domains and PDZ binding motif are shaded. (B) RTPCR analysis showing the temporal expression patterns of March2 in Xenopus development. Developmental stages are indicated above the lanes. ODC serves as a loading control. (C-S) Whole mount In situ hybridization assay showing the spatial expression patterns of March2. Lateral view at 4-cell stage (C) and stage 9 (D); vegetal (E) and bisected (F) view at stage 10; with an enlarged view showing dorsal mesoderm expression (G); vegetal (H) and bisected (I) view at stage 11; with an enlarged view showing dorsal mesoderm expression including the dorsal organizer region (J); anterior (K) and bisected (L, dorsal on right) view at stage 12; anterior view at stage 14 (M); anterior (N) and lateral (O, anterior on left) view at stage 20; lateral view at stage 23 (P, anterior on left); lateral view at stage 27 (Q); lateral view at stage 36 (R); with an enlarged view indicating expression in the heart region (S); dorsal blastopore lip (dl) is indicated; dashed lines indicates boundary of ectoderm (e) and mesoderm (m); arrows indicate anterior neural plate; arrowheads indicate heart (h). (T) RT-PCR analysis showing ubiquitous March2 expression in both animal and marginal regions at st.10.5 embryos. Xbra, pan-mesodermal marker; Chd, dorsal mesodermal marker; Msx1, animal and ventral mesodermal marker; WE and –RT, control RT-PCR on the whole embryo RNA in the presence or absence of reverse transcriptase; AC, animal cap cells; DMZ, dorsal marginal zone cells; VMZ, ventral marginal zone cells. (U) March2 protein is ubiquitously expressed during *Xenopus* embryogenesis. Embryos at indicated stages were subjected to Western blotting with anti-March2 antibody.

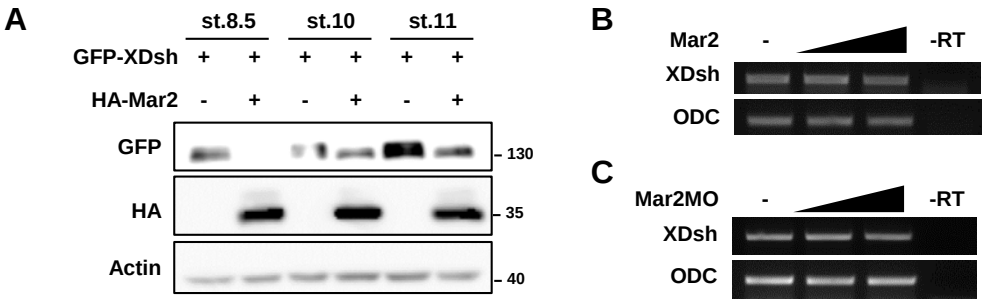

Fig. S2. March2 mediates Dsh degradation during *Xenopus* early embryogenesis without affecting transcription of Dsh (A) March2 decreases Dsh protein level at late blastula (stage 8.5) and gastrula (stage 10 and stage 11) embryos. GFP-XDsh mRNA (200pg) with or without HA-Mar2 (2ng) were injected as indicated and subjected to western blot analysis. (B,C) March expression or depletion do not affect transcription of Dsh mRNA. RT-PCR was performed using *Xenopus* stage 10.5 embryos with increasing amount of March2 mRNA injection (0.5ng and 1ng, respectively) (B) or March2 MO injection (20ng and 40ng, respectively) (C).

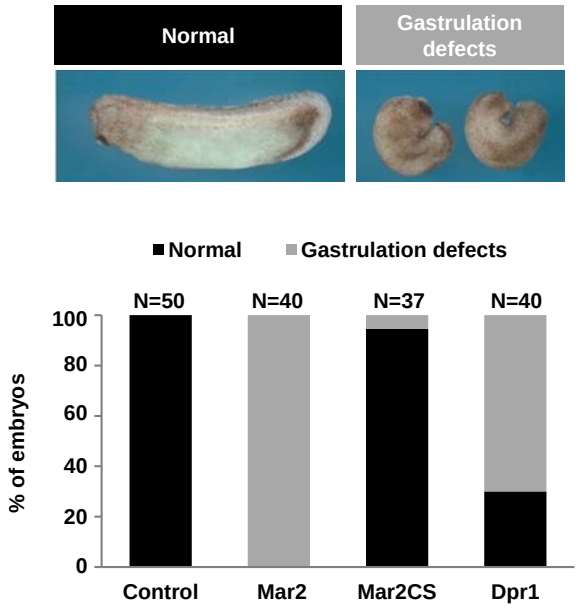

Fig. S3. Ectopic expressions of March2 and Dpr1 show phenocopies of Dsh morphants

Overexpression of both March2 and Dpr1 mRNA caused gastrulation defects including bended dorsal axis and opened blastopores. The amounts of injected reagents as follows: March2 WT and CS mRNA, 1ng, respectively; Dpr1 mRNA, 2ng.

A

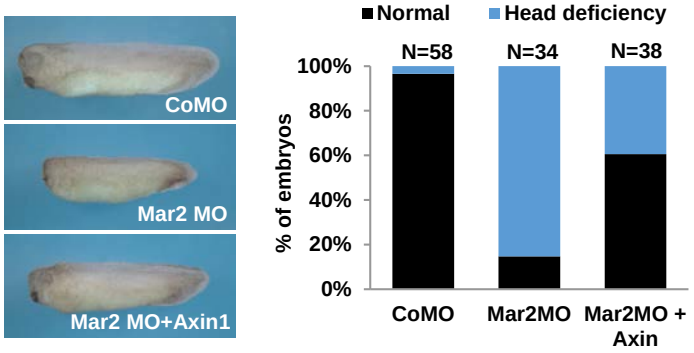

B

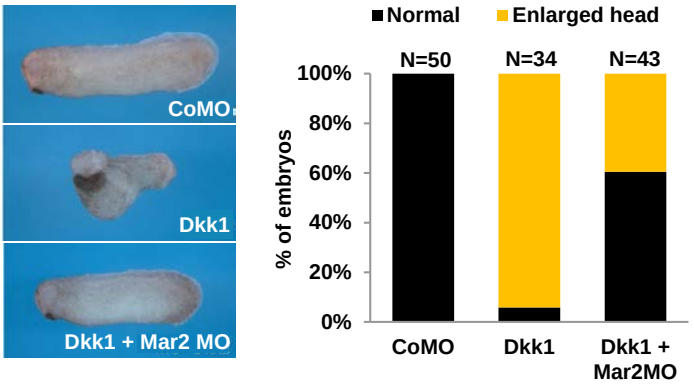

C

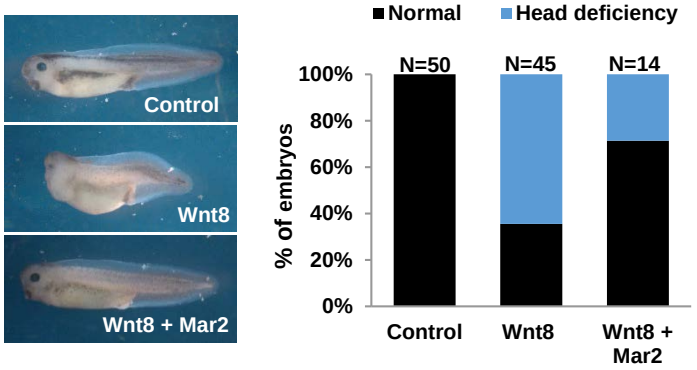

D

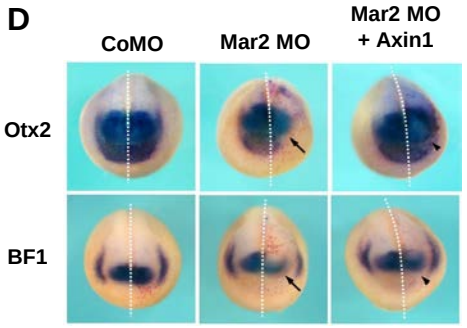

Fig. S4. March2 is required for the anterior head formation by antagonizing Wnt signaling pathway (A) The anterior head defect caused by Mar2 MO (40ng) was rescued by co-expression of Wnt negative regulator Axin1 mRNA (1ng). (B) Enlarged head induced by Wnt antagonist Dkk1 mRNA (25pg) was rescued by Mar2 MO (40ng). (C) The anterior head defect caused by Wnt8 DNA was rescued by co-expression of Mar2 mRNA. See Supplemental Table 3 for statistical data. (D) Reduction of Otx2 and BF1 expressions by Mar2MO (40ng) could be restored by coexpression of Axin1 mRNA. β-galactosidase mRNA (100pg) was co-injected as a lineage tracer. Right sides of the embryos represented are injected with indicated reagents.

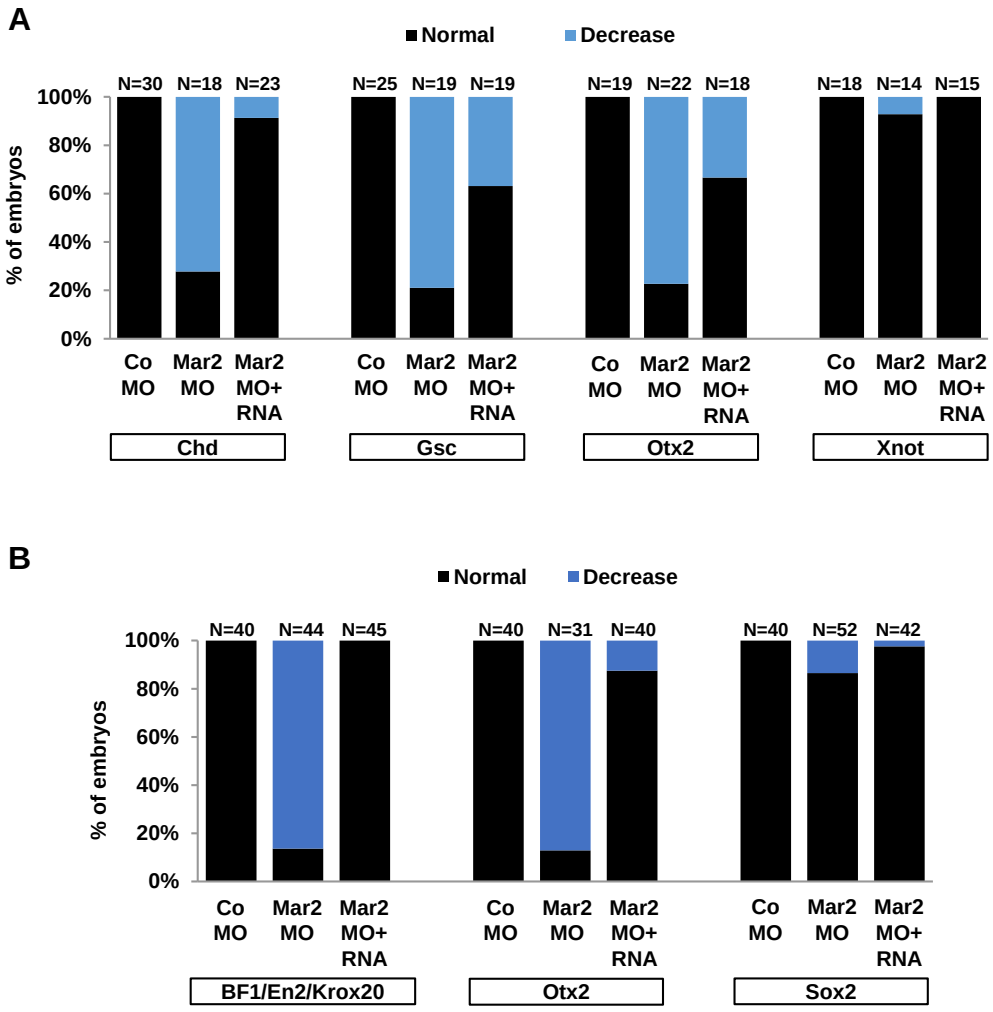

Fig. S5. Quantification analyses of Fig. 5C and Fig. 5D. See Tables S3 for statistical data.

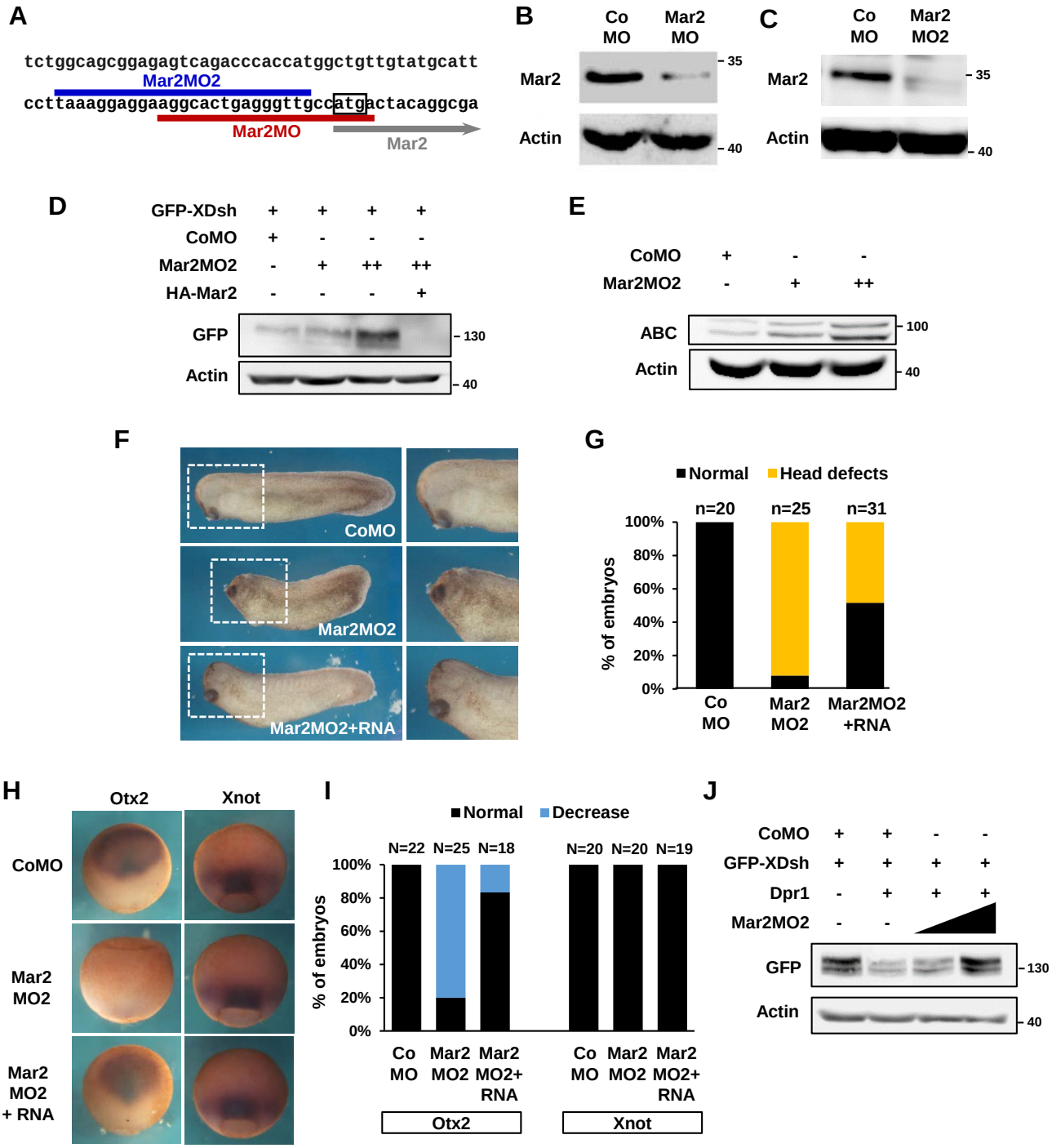

Fig. S6. March2MO2 mediates Dsh degradation and is required for anterior head formation.

(A) Cartoon representation of two Antisense Morphorlino oligonucleotides of March2 (MO and MO2) binding sites and MO-resistant form of March2 mRNA (HA-Mar2). Start codon is indicated with the box. (B, C) The efficacy of Mar2MO and Mar2MO2 inhibiting March2 protein synthesis. 4-cell stage *Xenopus* embryos were injected with 40ng of CoMO or Mar2MOs and subjected to western blot with anti-March2 antibody at stage 12. (D) Mar2MO2 stabilizes Dsh protein. Mar2MO2 (40, 80ng) were injected respectively with 150pg of GFP-XDsh mRNA. Co-injection of 500pg of March2 mRNA along with 80ng of Mar2MO reduced Dsh again. (E) Mar2MO2 mediates activation of β-catenin (ABC). Four-cell stage embryos were dorsally injected with CoMO or Mar2MO2 (40ng, 80ng) and analyzed at stage 10.5. Actin as loading controls. (F) Dorso-animal injection of Mar2MO2 (40ng) at eight-cell stage results defects in anterior head formation, and these defects were rescued by co-expression of a MO-resistant form of Xenopus March2 mRNA (500pg). (G) Quantification of (F). (H) In situ hybridization analysis showing that Mar2MO2 (40ng) suppresses expressions of Otx2 at stage 12 but does not suppress Xnot at stage 11.5 Co-expression of March2 mRNA (500pg) rescues reduction of these genes. (I) Quantification of (H). (J) Mar2MO2 inhibits Dpr1-mediated decrease of Dsh. Amounts of injected mRNAs and MOs: GFP-XDsh, 200pg; CoMO, 80ng; and Mar2MO, 40ng and 80ng; Dpr1, 2ng.

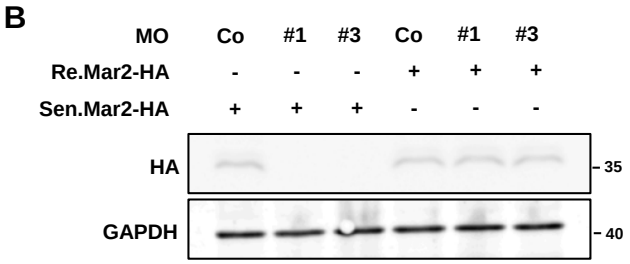

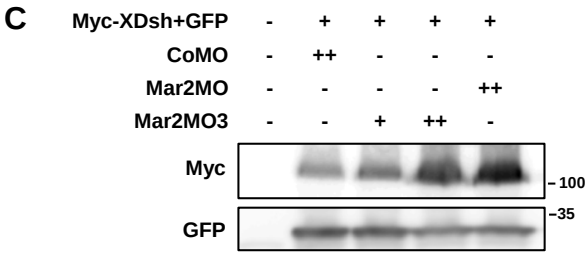

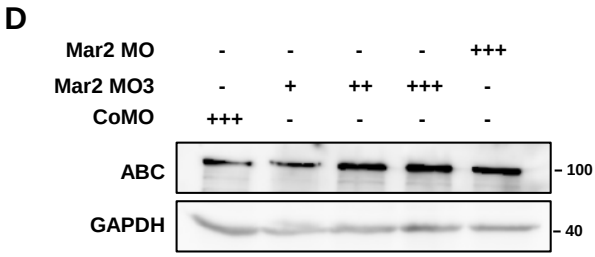

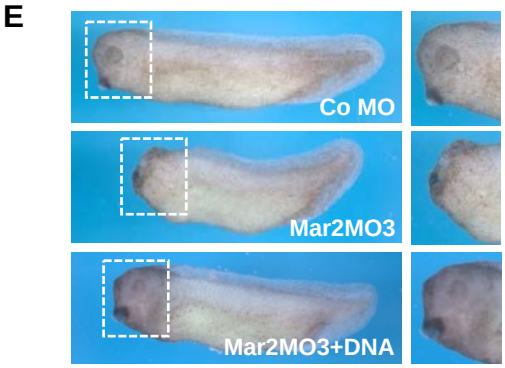

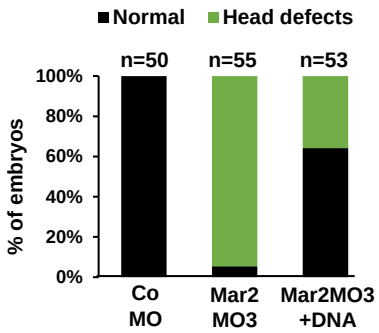

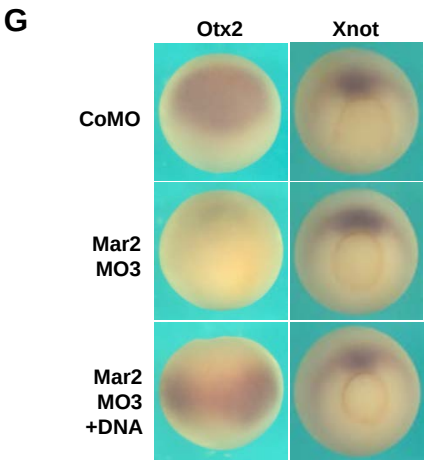

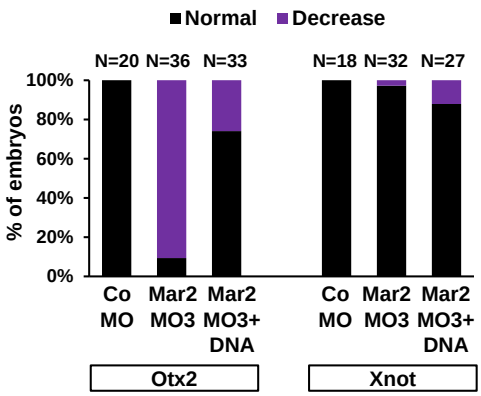

Fig. S7. Non-overlapping March2MO3 mediates Dsh degradation and is required for anterior head formation.

(A) Cartoon representation of all Antisense Morphorlino oligonucleotides of March2 (MO, MO2, and MO3) binding sites and MO-resistant form of March2 mRNA (HA-Mar2). Start codon is indicated with the box. Note that MO3 is not overlapped with other March2 MOs. (B) Western blot analysis showing the efficacy and specificity of Mach2 MO and MO3. Embryos co-injected with March2 MOs (20 ng) and MO-resistant (Re) March2-HA (200 pg) or MO-sensitive(Sen) March2-HA (200 pg) were subjected to Western blotting with anti-Myc antibody. Sen.Mar2-HA depicts HA-tagged with open reading frame (ORF) containing partial untranslated region (UTR) which is provided to the target of March2 MOs. Re.Mar2-HA is an off-target construct lacking UTR. (C) Mar2MO3 stabilizes Dsh protein in a dosage-dependent manner. Mar2MO (80ng) or Mar2MO3 (40, 80ng) were injected respectively with 200pg of Myc-XDsh mRNA and GFP. (D) Mar2MO3 mediates activation of β-catenin (ABC). Eight-cell stage embryos were dorsally injected with CoMO, Mar2MO (80ng), or Mar2MO3 (20ng, 40ng, 80ng) and analyzed at stage 10.5. GAPDH as loading controls. (E) Dorso-animal injection of Mar2MO3 (40ng) at eight-cell stage results defects in anterior head formation, and these defects were rescued by co-expression of a Xenopus March2 DNA (50pg). (F) Quantification of (E). (G) In situ hybridization analysis showing that Mar2MO3 (40ng) suppresses expressions of Otx2 at stage 12 but does not suppress Xnot at stage 11.5 Co-expression of March2 DNA (50pg) rescues reduction of these genes. (H) Quantification of (G).

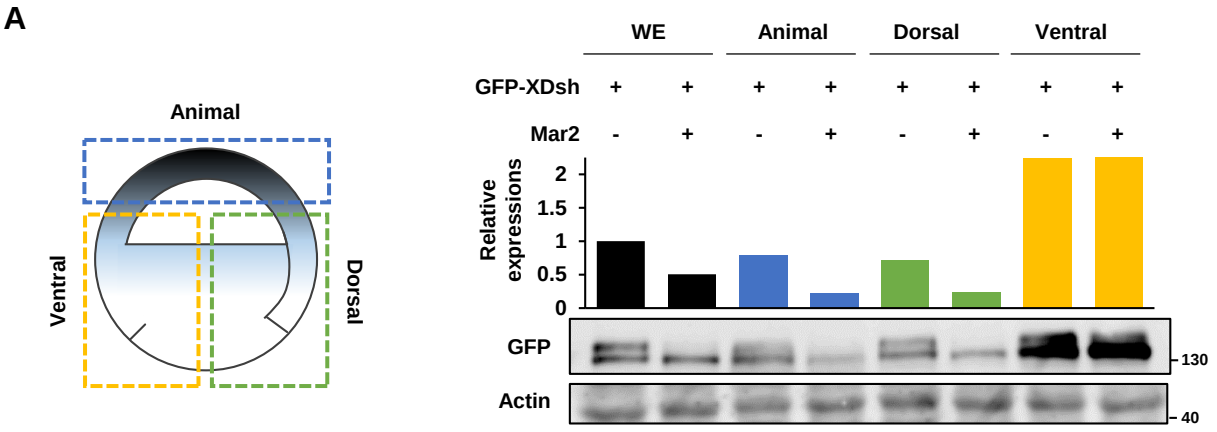

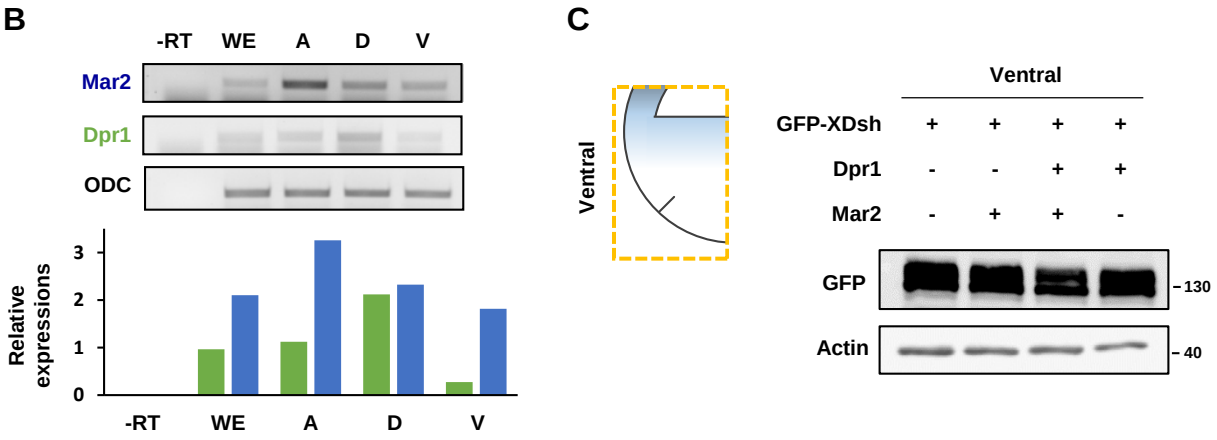

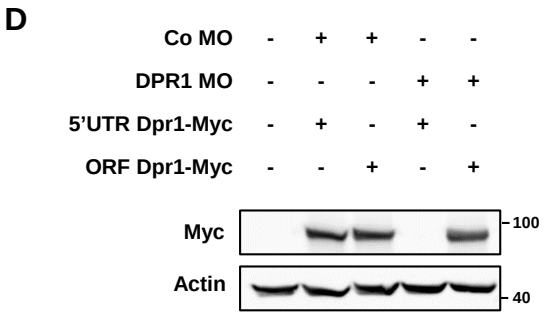

Fig. S8. Dapper1 gives dorso-animal specificity for March2 functions of Dsh degradation

(A) March2 mediates Dsh degradation at animal and dorsal regions of gastrula embryos. GFP-XDsh (200pg) and HA-Mar2 (1ng) were injected at the animal, dorsal and ventral regions of the four-cell stage embryos, respectively. Each regions were dissected at stage 10.5, cultured until stage 11 and subjected to Western blot analysis. Graph shows quantification of band intensities. (B) Expressions of March2 and Dpr1 transcripts at animal (A), dorsal (D) and ventral (V) regions of gastrula embryo. RT-PCR analysis showed that March2 is expressed ubiquitously at all regions, whereas Dpr1 is majorly expressed at the dorsal region of the embryo. Graph shows quantification of band intensities. (C) A sub-optimal dosage of Dpr1 mRNA expression at ventral region enables March2 mediated Dsh degradation. Dpr1 mRNA (500pg) were injected with March2 mRNA (1ng) at the ventral region of four-cell stage embryos. Ventral regions were dissected at stage 10.5 and cultured until stage 11 and analyzed with the Western blotting. (D) Western blot analysis showing the efficacy and specificity of Dpr1 MO. Embryos co-injected with Dpr1 MO (40 ng) and 5'UTR Dpr1-Myc (500 pg) or ORF Dpr1-Myc (500 pg) were subjected to Western blotting with anti-Myc antibody. UTR-Dpr1- Myc depicts Myc-tagged Dpr1 open reading frame (ORF) containing partial untranslated region (UTR) which is provided to the target of Dpr1 MO. ORF-Dpr1-Myc is an off-target construct lacking UTR.

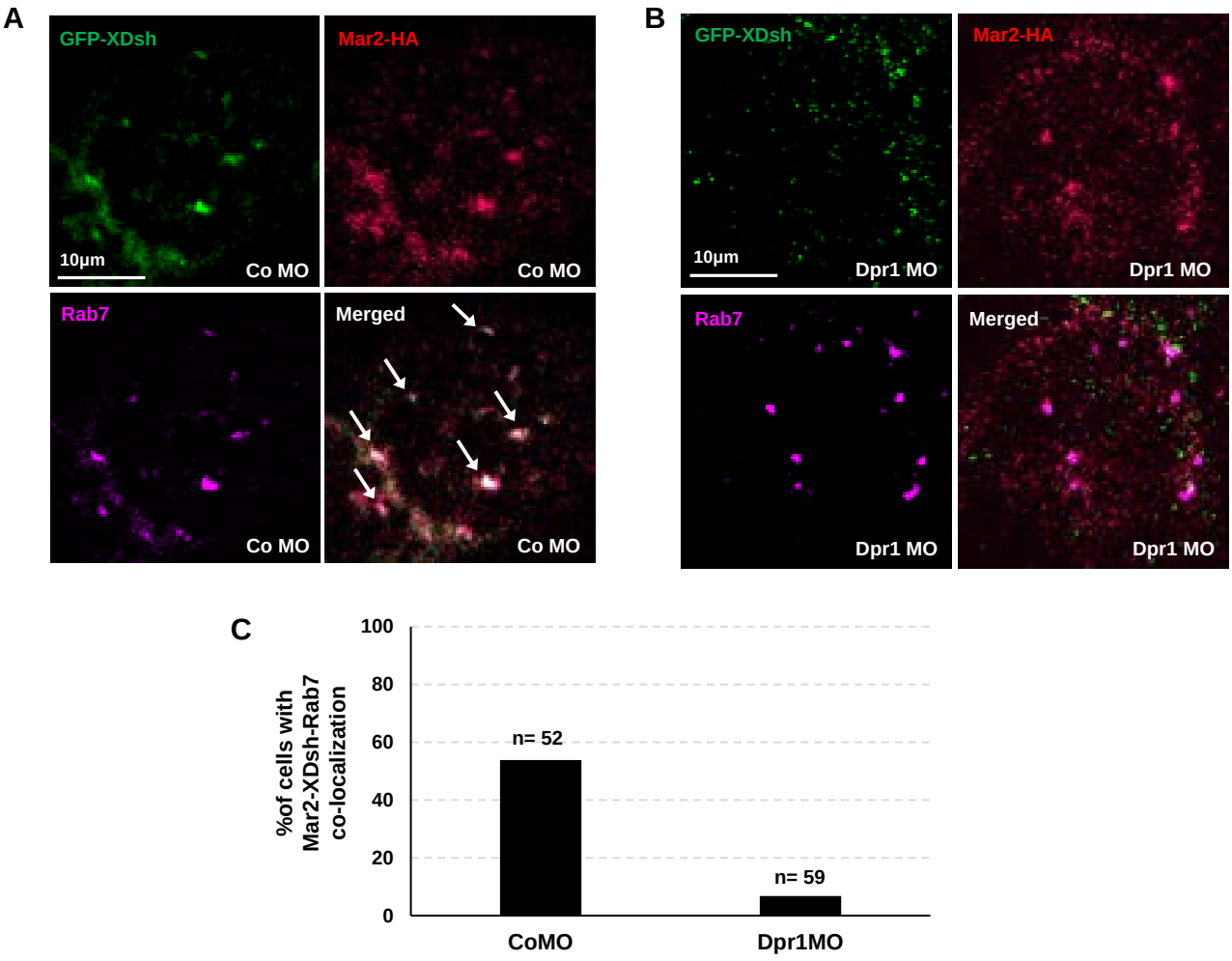

Fig. S9. Dapper1 is required for recruitment of Dsh to March2 in lysosomes

(A, B) Confocal images showing the subcellular localization of GFP-Dsh (2ng) and March2-HA (500pg) in control MO injected (40ng) (A) or Dpr1 MO injected (40ng) (B) *Xenopus* animal cap tissues. Endogenous Rab7 was co-stained for lysosomes. White arrows indicate co-localized puncta of March2, Dsh and Rab7. Note that depletion of Dpr1 by MO (B) eliminated co-localization of Dsh with Rab7-positive March2 puncta. (C) Quantification of (A) and (B).

Supplementary Tables

Table S1. Antibodies

	Manufacturer	Catalog #	Dilutions used
Activated β-catenin Antibody	Millipore	#05-665	1:1000
Human Dvl-1 Antibody	Santa Cruz	#sc-8025	1:1000
Actin Antibody	Santa Cruz	#sc-1666-R	1:2000
HA Antibody	Santa Cruz	#sc-7392, sc-805	1:1000~2000
GFP Antibody	Santa Cruz	#sc-9996	1:1000~2000
Myc Antibody	Santa Cruz	#sc-789, sc-40	1:1000~2000
Flag Antibody	Sigma	#F3165	1:1000~2000
EEA1 Antibody	Abcam	#ab2900	1:250
Rab7 Antibody	Cell Signaling	#9367	1:250
Lamp1 Antibody	Abcam	#ab24170	1:200
Phospho-LRP6 (Ser1490) Antibody	Cell Signaling	#2568	1:1000
LRP6 (C5C7) Antibody	Cell Signaling	#2560	1:1000
Alexa Fluor 594 goat anti-mouse IgG	Life Technologies	#A11005	1:250
Alexa Fluor 647 donkey anti-rabbit IgG	Life Technologies	#A31573	1:250
Mouse March2 antibody	Gift from Dr. Hirose (Nakamura et al., 2005)		For Immunoblotting: 1:500 For Immunofluorescence: 1:200

Validation profiles of all commertial antibodies are available from manufacturers' datasheets. Dilution of the antibodies was followed by the manufacturers'application guidelines.

Nakamura, N., Fukuda, H., Kato, A., and Hirose, S. (2005). MARCH-II is a syntaxin-6-binding protein involved in endosomal trafficking. Molecular biology of the cell *16*, 1696-1710.

Table S2. Lists of top 50 Dsh interacting candidates from bioinformatics analysis

Rank	C term	Score	Description
1	EWYV	7.19	O57311|ZIC3_XENLA Zinc finger protein ZIC 3 - Xenopus laevis
1	EWYV	7.19	Q91689|ZIC2_XENLA Zinc finger protein ZIC 2 - Xenopus laevis
1	EWYV	7.19	O73689|ZIC1_XENLA Zinc finger protein ZIC 1 - Xenopus laevis
4	ITFV	7.02	Q7ZXB1|MCM7B_XENLA DNA replication licensing factor mcm7-B - Xenopus laevis
4	ITFV	7.02	Q91876|MCM7A_XENLA DNA replication licensing factor mcm7-A - Xenopus laevis
6	LTFV	6.41	Q2KHS5|MOG2A_XENLA 2-acylglycerol O-acyltransferase 2-A - Xenopus laevis
7	EYFI	5.92	Q7ZXX1|_XENLA Cell adhesion molecule 3 precursor - Xenopus laevis
8	NYFV	5.88	Q68F68|TOR2A_XENLA Torsin-2A precursor - Xenopus laevis
9	SAFL	5.48	Q7ZWW7|TS31B_XENLA Tetraspanin-31-B - Xenopus laevis
9	SAFL	5.48	Q5XHG6|TS31A_XENLA Tetraspanin-31-A - Xenopus laevis
11	STFL	5.35	P47827|CCNA2_XENLA Cyclin-A2 - Xenopus laevis
12	SSFL	4.94	Q5HZM3|BAFL_XENLA Barrier-to-autointegration factor-like protein - Xenopus laevis
13	EFFI	4.44	Q66KX2|CADM4_XENLA Cell adhesion molecule 4 precursor - Xenopus laevis
14	ASFV	4.44	Q8AVG9|QRSL1_XENLA Gln-tRNA amidotransferase subunit A homolog - Xenopus laevis
15	DYFL	3.82	Q6IP91|PP4C_XENLA Serine/threonine-protein phosphatase 4 catalytic subunit - Xenopus laevis
16	ETTV	3.76	Q5PQ35|MARH2_XENLA E3 ubiquitin-protein ligase MARCH2 - Xenopus laevis
16	ETTV	3.76	Q9PUU6|FZD2_XENLA Frizzled-2 precursor - Xenopus laevis
16	ETTV	3.76	Q9I9M5|FZD1_XENLA Frizzled-1 precursor - Xenopus laevis
19	PYLV	3.76	P35668|GSHB_XENLA Glutathione synthetase - Xenopus laevis
20	DAFL	3.26	Q66KV4|BAFB_XENLA Barrier-to-autointegration factor B - Xenopus laevis
20	DAFL	3.26	Q6NTS2|BAFA_XENLA Barrier-to-autointegration factor A - Xenopus laevis
22	ETSV	3.23	Q90Z05|VNG2B_XENLA Vang-like protein 2-B - Xenopus laevis
22	ETSV	3.23	Q90X64|VNG2A_XENLA Vang-like protein 2-A - Xenopus laevis
24	GLFF	3.14	P03912|NU4M_XENLA NADH-ubiquinone oxidoreductase chain 4 - Xenopus laevis
24	GLFF	3.14	Q6NUC2|CSN6_XENLA COP9 signalosome complex subunit 6 - Xenopus laevis
26	IALL	3.12	Q3BJS1|FOXN4_XENLA Forkhead box protein N4 - Xenopus laevis
27	ETLL	3.10	Q32NH9|FXJ12_XENLA Forkhead box protein J1.2 - Xenopus laevis
28	ELRV	3.05	Q08B84|RN19B_XENLA E3 ubiquitin-protein ligase RNF19B - Xenopus laevis
28	ELLV	3.05	Q5EAU9|FA82C_XENLA Protein FAM82C - Xenopus laevis
30	EAEL	2.87	Q6INL2|KLH30_XENLA Kelch-like protein 30 - Xenopus laevis
31	GEV	2.80	Q7ZYQ0|FXI1E_XENLA Forkhead box protein I1-ema - Xenopus laevis
32	QEAK	2.80	NP_001089066.1| Ubiquitin carboxyl-terminal hydrolase L5 - Xenopus laevis

33	DSFL	2.72	P26619|PGFRA_XENLA Alpha-type platelet-derived growth factor receptor - Xenopus laevis
34	ISSV	2.71	Q66IW8|BRF2_XENLA Transcription factor IIIB 50 kDa subunit - Xenopus laevis
35	EFYI	2.66	Q6GQ34|F124A_XENLA Protein FAM124A - Xenopus laevis
36	EAFK	2.66	P21783|NOTCH_XENLA Neurogenic locus notch protein homolog precursor - Xenopus laevis
37	GTQV	2.53	Q58E76|ATD3A_XENLA ATPase family AAA domain-containing protein 3-A - Xenopus laevis
38	ETFH	2.53	Q6PA69|DEFI6_XENLA Differentially expressed in FDCP 6 homolog - Xenopus laevis
39	LTDV	2.41	P22739|KCNA2_XENLA K+ voltage-gated channel subfamily A member 2 - Xenopus laevis
40	ETWS	2.39	Q6NRG5|NDOR1_XENLA NADPH-dependent diflavin oxidoreductase 1 - Xenopus laevis
41	GSEV	2.38	Q8JIT5|FXI1C_XENLA Forkhead box protein I1c - Xenopus laevis
42	LSQV	2.38	O93274|FZD8_XENLA Frizzled-8 precursor - Xenopus laevis
43	SYWY	2.33	Q6GPM4|RM24_XENLA 39S ribosomal protein L24, mitochondrial precursor - Xenopus laevis
44	ILQV	2.32	Q5XH39|MARH8_XENLA E3 ubiquitin-protein ligase MARCH8 - Xenopus laevis
45	PSGV	2.31	Q6P6Z4|CK2N2_XENLA Ca^{2+}/CAM-dependent protein kinase II inhibitor 2 - Xenopus laevis
46	SLLV	2.30	O57428|HASS_XENLA Hyaluronan synthase-related protein - Xenopus laevis
47	GYFK	2.25	Q641I1|F135B_XENLA Protein FAM135B - Xenopus laevis
48	ETLI	2.23	Q9PT60|RBP1A_XENLA RalA-binding protein 1-A - Xenopus laevis
49	LATL	2.16	Q6DF87|TM170_XENLA Transmembrane protein 170 - Xenopus laevis
50	PHFV	2.13	Q6DE55|HMHA1_XENLA Minor histocompatibility protein HA-1 - Xenopus laevis

Tables S3. Statistical Analysis

Figure. 4E.

	Normal	Partial	Full	Total
CoMO	50	0	0	50
CoMO+Wnt8	29	9	9	47
Mar2MO+Wnt8	16	12	10	38
	Normal	Partial	Full	Total
CoMO	30	0	0	30
CoMO+Wnt8	15	6	4	25
Mar2MO+Wnt8	12	12	6	30
	Normal	Partial	Full	Total
CoMO	30	0	0	30
CoMO+Wnt8	20	10	6	36
Mar2MO+Wnt8	10	8	7	25

Figure. 5F.

	Normal	Head defects	CE defects	Total
CoMO	30	0	0	30
Mar2MO	4	38	5	47
XDshMO	25	1	2	28
Mar2MO+XDshMO	26	26	2	54
CoMO	30	0	0	30
Mar2MO	1	28	2	31
XDshMO	25	2	2	29
Mar2MO+XDshMO	13	17	5	35
CoMO	20	0	0	20
Mar2MO	3	32	7	42
XDshMO	17	1	3	21
Mar2MO+XDshMO	9	10	0	19

Figure 7D.

	Normal	Head defects	Gastrulation defects	Total
CoMO	50	0	0	50
Mar2MO	29	3	0	32
Dpr1MO	36	3	0	39
Mar2MO+Dpr1MO	17	16	3	36

Figure S3.

	Normal	Gastrulation defects	Total
Control	50	0	50
Mar2WT	0	40	40
Mar2CS	35	2	37
Dpr1	12	28	40

Figure 5B.

	Normal	Head defects	Total
CoMO	50	0	50
Mar2MO	3	27	30
MO +RNA	26	12	38

Figure 5E.

	Normal	Head defects	CE defects	Total
CoMO	30	0	0	30
Mar2MO (20ng)	16	4	1	21
XDsh	23	3	3	29
Mar2MO (20ng) + XDsh	13	15	2	30

Figure. 7C.

	Normal	Mild	Severe	Total
CoMO	50	0	0	50
Wnt8	2	12	38	52
Wnt8+Mar2	16	18	12	46
Wnt8+Mar2 +Dpr1MO	0	21	29	50
	Normal	Mild	Severe	Total
CoMO	30	0	0	30
Wnt8	0	8	22	30
Wnt8+Mar2	8	11	10	29
Wnt8+Mar2 +Dpr1MO	0	6	25	31
	Normal	Mild	Severe	Total
CoMO	50	0	0	50
Wnt8	4	12	20	36
Wnt8+Mar2	13	19	8	40
Wnt8+Mar2 +Dpr1MO	0	19	21	40

Figure S4A.

	Normal	Head defects	Total
CoMO	56	2	58
Mar2MO	5	29	34
MO +Axin	23	15	38

Figure S4B.

	Normal	Enlarged head	Total
CoMO	50	0	50
Dkk1	2	32	34
Dkk1+MO	26	17	43

Figure S4C.

	Normal	Head defects	Total
CoMO	50	0	50
Wnt8	29	16	45
Wnt8+Mar2	10	4	14

Figure S5A.

	Chd			Gsc			Otx2			Xnot		
	Normal	Decrease	Total	Normal	Decrease	Total	Normal	Decrease	Total	Normal	Decrease	Total
Con	30	0	30	25	0	25	19	0	19	18	0	18
Mar2MO	13	5	18	4	15	19	5	17	22	13	1	14
MO+RNA	21	2	23	12	7	19	12	6	18	15	0	15

Figure S5B.

	BF1/En2/Krox20			Otx2			Sox2		
	Normal	Decrease	Total	Normal	Decrease	Total	Normal	Decrease	Total
Con	40	0	40	40	0	40	40	0	40
Mar2MO	6	38	44	4	27	31	45	7	52
MO+RNA	45	0	45	35	5	40	41	1	42

Figure. S6G

	Normal	Head defects	Total
CoMO	20	0	20
Mar2MO2	2	23	25
Mar2MO2+RNA	16	15	31

Figure. S6I

Otx2	Normal	Decrease
CoMO	22	0
Mar2MO2	5	20
MO2+RNA	15	3
Xnot	**Normal**	**Decrease**
CoMO	20	0
Mar2MO2	20	0
MO2+RNA	19	0

Table S4. Primers for RT-PCR

ODC	Forward	5'-CAG CTA GCT GTG GTG TGG-3'
	Reverse	5'-CAA CAT GGA AAC TCA CAC C-3'
Xbra	Forward	5'- GCT GGA AGT ATG TGA ATG GAG -3'
	Reverse	5'-TTA AGT GCT GTA ATC TCT TCA -3'
Siamois	Forward	5' AAG ATA ACT GGC ATT CCT GAG C 3'
	Reverse	5' GGT AGG GCT GTG TAT TTG AAG G 3'
Xnr-3	Forward	5' -CGA GTG CAA GAA GGT GGA CA- 3'
	Reverse	5'- ATC TTC ATG GGG ACA CAG GA- 3'
Chordin	Forward	5'-CCT CCA ATC CAA GAC TCC AGC AG-3'
	Reverse	5'-GGA GGA GGA GGA GCT TTG GGA CAA G-3’
Msx-1	Forward	5'-GCT AAA AAT GGC TGC TAA-3'
	Reverse	5'-AGG TGG GCT GTG TAA AGT-3'

Reference: http://www.hhmi.ucla.edu/derobertis/